mathematics

MDPI

Article

Enhancing Robustness in Precast Modular Frame Optimization: Integrating NSGA-II, NSGA-III, and RVEA for Sustainable Infrastructure

Andrés Ruiz-Vélez [1], José García [2], Julián Alcalá [1] and Víctor Yepes [1,*]

[1] Institute of Concrete Science and Technology (ICITECH), Universitat Politècnica de València, 46022 València, Spain; aruivel@doctor.upv.es (A.R.-V.); jualgon@upv.es (J.A.)
[2] School of Construction and Transportation Engineering, Pontificia Universidad Católica de Valparaíso, Valparaíso 2362804, Chile; jose.garcia@pucv.cl
* Correspondence: vyepesp@cst.upv.es

Abstract: The advancement toward sustainable infrastructure presents complex multi-objective optimization (MOO) challenges. This paper expands the current understanding of design frameworks that balance cost, environmental impacts, social factors, and structural integrity. Integrating MOO with multi-criteria decision-making (MCDM), the study targets enhancements in life cycle sustainability for complex engineering projects using precast modular road frames. Three advanced evolutionary algorithms—NSGA-II, NSGA-III, and RVEA—are optimized and deployed to address sustainability objectives under performance constraints. The efficacy of these algorithms is gauged through a comparative analysis, and a robust MCDM approach is applied to nine non-dominated solutions, employing SAW, FUCA, TOPSIS, PROMETHEE, and VIKOR decision-making techniques. An entropy theory-based method ensures systematic, unbiased criteria weighting, augmenting the framework's capacity to pinpoint designs balancing life cycle sustainability. The results reveal that NSGA-III is the algorithm converging towards the most cost-effective solutions, surpassing NSGA-II and RVEA by 21.11% and 10.07%, respectively, while maintaining balanced environmental and social impacts. The RVEA achieves up to 15.94% greater environmental efficiency than its counterparts. The analysis of non-dominated solutions identifies the A_4 design, utilizing 35 MPa concrete and B500S steel, as the most sustainable alternative across 80% of decision-making algorithms. The ranking correlation coefficients above 0.94 demonstrate consistency among decision-making techniques, underscoring the robustness of the integrated MOO and MCDM framework. The results in this paper expand the understanding of the applicability of novel techniques for enhancing engineering practices and advocate for a comprehensive strategy that employs advanced MOO algorithms and MCDM to enhance sustainable infrastructure development.

Keywords: multi-objective optimization; multi-criteria decision-making; NSGA-II; NSGA-III; RVEA; SAW; FUCA; TOPSIS; PROMETHEE; VIKOR

MSC: 90C11; 90C27; 90C29

Citation: Ruiz-Vélez, A.; García, J.; Alcalá, J.; Yepes, V. Enhancing Robustness in Precast Modular Frame Optimization: Integrating NSGA-II, NSGA-III, and RVEA for Sustainable Infrastructure. *Mathematics* **2024**, *12*, 1478. https://doi.org/10.3390/math12101478

Academic Editor: Anna Sciomachen

Received: 2 April 2024
Revised: 6 May 2024
Accepted: 8 May 2024
Published: 9 May 2024

1. Introduction

Transportation infrastructure stands as the most pivotal component of a nation's core infrastructure, often representing its largest subcomponent and serving as a critical foundation for economic prosperity and societal welfare. The allocation of resources towards this sector is perceived as a direct contribution to a nation's economic and social growth, evidenced by leading institutions such as the World Bank allocating substantial financial support to transportation infrastructure, surpassing contributions towards health or education [1]. This strategic emphasis highlights transportation infrastructure's crucial role in

catalyzing societal progression. Amidst an increasingly marked transition towards sustainable development, the investment strategy in transportation infrastructure now necessitates a holistic life cycle evaluation [2]. This approach ensures that fiscal commitments address immediate needs and champion enduring, sustainable solutions that protect future generations' interests. It integrates environmental sustainability and global interconnectivity into the essence of infrastructure development, fostering a paradigm that balances immediate benefits with long-term viability.

Within the crucial role of transportation infrastructure, the construction sector stands as a dynamic catalyst, essential for the fruition of these projects. The construction industry is poised for substantial growth, with forecasts indicating a surge beyond 14 trillion dollars globally in the ensuing year, significantly influencing the global economic landscape [3]. This expansion illustrates the industry's immense scale and its vital role in propelling economic advancement through the generation of employment opportunities, both during the design and construction phases and in the ongoing maintenance of infrastructure. Its operation strengthens job prospects within the sector and related fields, underscoring the construction industry's contribution to broad-based economic development.

However, positioned as one of the most resource-intensive and environmentally impacting sectors, the construction industry is under increasing scrutiny to reform antiquated practices in favor of more sustainable approaches [4]. This juxtaposition of the industry's considerable economic contributions against its environmental and social implications has sparked a critical examination. Acknowledging this challenge has prompted a realignment of capital investment strategies, prioritizing incorporating life cycle sustainability—encompassing economic, environmental, and social considerations—right from the conceptual stages of transportation infrastructure projects [5]. This shift is not merely a nod to ethical standards but emerges as a strategic necessity to secure investment and champion the cause of sustainable development. The construction sector is compelled to embrace a comprehensive strategy that transcends traditional methodologies. Adopting an integrated approach in designing highly efficient infrastructure is instrumental in realizing economically sound, environmentally sustainable, and socially equitable projects, marking a significant stride towards a balanced development paradigm.

Adopting an integrated framework incorporating sustainable design strategies from the outset is essential for aligning transportation infrastructure construction with overarching sustainable development objectives [6]. This strategy ensures that efforts in construction engineering are developed with a comprehensive outlook, evaluating aspects such as economic viability, environmental preservation, and social responsibility. Embracing this broader framework, which considers the project's entire life cycle, can stimulate innovation and foster more profound collaboration among all stakeholders. Moreover, it sets a foundational standard for integrating life cycle sustainability considerations, facilitating more enlightened decision-making throughout the critical phases of conception, design, and funding acquisition of transportation infrastructure projects. This refined approach ensures the immediate project needs are met while incorporating a shift towards more responsible and forward-thinking infrastructure development practices.

Embracing a life cycle standpoint necessitates the evaluation and objective quantification of environmental, social, and economic impacts spanning from a project's inception to its decommissioning. This perspective fosters sensitive material and energy use, emphasizing long-term benefits for communities and the environment. Applying advanced life cycle and structural mathematical modeling signifies a pivotal transition from traditional to innovative design strategies. This shift promotes the early integration of optimization and decision-making techniques, significantly enhancing the alignment of infrastructure projects with sustainable development goals. Such an approach underlines the importance of a holistic view in infrastructure development, ensuring that projects are not only designed for immediate functionality under economic viability constraints but also for their long-term sustainability, operational efficiency, and positive societal impact throughout their entire life cycle.

The transition from single-objective optimization (SOO) to MOO in the context of structural design optimization signifies a substantial advancement [7–9]. MOO enables the simultaneous evaluation of multiple critical factors, including economic efficiency, environmental sustainability, and social impact. This holistic approach broadens the scope of design considerations and ensures a deeper congruence between infrastructure design and overarching sustainable development purposes. The advancement of MOO strategies represents a paradigmatic evolution, enriching the design process with a multifaceted perspective that better captures the complexity of real-world engineering challenges.

In Ruiz-Velez et al. [10], a novel design strategy is presented and applied to a real-world challenge in construction engineering. The study specifically focuses on the life cycle design optimization of reinforced concrete precast modular frames (RCPMF). Building on previous SOO results for the precast and cast-in-place typologies [11,12], the study introduces a customized non-dominated sorting genetic algorithm II (NSGA-II), enhanced with three novel repair operators, to navigate the complex handling of the mixed integer programming (MIP) during the optimization process [13]. Furthermore, the framework proposed in the study is particularly relevant for its integration with MCDM techniques, computing the criteria weights via an entropy-based approach and applying the simple additive weighting (SAW) and faire un choix adéquat (FUCA) methods for assessing the optimization results [14].

The statistical-based repair operator was identified as the preeminent algorithm for navigating the hurdles intrinsic to the MIP nature of the RCPMF optimization problem. Despite the inherent differences in the strategies for scoring and evaluating decision-making alternatives, the SAW and FUCA techniques ranked the optimal solutions similarly. This consistency attests to the capabilities of the proposed structural design framework and the potential of integrating MOO and MCDM. As a result, the study introduced and demonstrated a pioneering framework that leverages the strengths of MOO and MCDM to elevate the sustainability and efficacy of structural engineering projects. The research strongly supports deploying this integrative strategy in practical structural engineering scenarios, particularly those aimed at enhancing the sustainability of transportation infrastructure projects.

Integrating MOO with MCDM techniques presents a forward-looking strategy for refining structural design frameworks considering the life cycle implications of construction projects. The case study on optimizing the structural design of RCPMF sets a reliable standard for assessing the effectiveness of sophisticated design strategies in transportation infrastructure development. The results of exploring the NSGA-II algorithm alongside SAW and FUCA techniques underscored the potential benefits of integrating MOO and MCDM for addressing the complex task of embedding sustainability into structural design engineering, representing an important stride towards further analytical advancements. Consequently, this initiates a pivotal conversation about exploring and evaluating the performance of additional MOO algorithms and MCDM approaches. This scrutiny seeks to assess the framework's efficacy and broaden its relevance throughout the structural design domain.

This paper focuses on the development stage of precast modular frames, adopting a comprehensive perspective on life cycle sustainability. By integrating optimization processes early in the foundational phase, the framework is conceived to significantly influence the entire life cycle—from inception to decommissioning—ensuring that every design decision upholds long-term sustainability objectives [15]. The research builds substantially upon previous efforts by incorporating a broad spectrum of MOO algorithms and MCDM techniques, enhancing the framework's ability to navigate the complex and multifaceted challenges common to diverse modern engineering projects and boosting its applicability and robustness.

Furthermore, by embedding life cycle sustainability objectives directly into the optimization process, aligning these objectives with decision-making criteria, and utilizing an entropy theory-based weighting method, the framework ensures robustness and impar-

tiality. This holistic approach deepens the understanding of life cycle sustainability and improves the replicability and reliability of outcomes across various engineering domains, fostering real-world scalability for these advanced practices. The research showcases the practical implementation of the MOO and MCDM integrated framework, closely aligning with established best practices for sustainable infrastructure development.

Within this context, the present research implements and critically evaluates the performance of novel MOO algorithms and MCDM techniques for enhancing structural design efforts. Three optimization algorithms and five decision-making techniques are implemented within the integrated design framework and then employed to solve the RCPMF problem. This paper aims to comprehensively characterize and enhance the integrated design strategy's capabilities for solving practical engineering challenges. This paper introduces and evaluates the performance of three novel MOO algorithms, NSGA-II, non-dominated sorting genetic algorithm III (NSGA-III), and reference vector guided evolutionary algorithm (RVEA), for solving the MOO RCPMF problem [16–19]. The statistical-based repair operator, previously identified as the best-performing repair algorithm, is implemented in all of them. This paper further innovates by substantially extending the scope of the MCDM problem by comparing five different decision-making techniques: SAW, FUCA, technique for order of preference by similarity to ideal solution (TOPSIS), preference ranking organization method for enrichment evaluation (PROMETHEE), and "visekriterijumska optimizacija i kompromisno resenje" (VIKOR), Serbian for multi-criteria optimization and compromise solution [20,21]. This exhaustive examination improves the understanding of the MOO and MCDM integrated life cycle design strategy's suitability and efficiency in promoting sustainable development within transportation infrastructure.

The NSGA-III algorithm is identified as the best-performing MOO strategy across all objective functions. While differing in scoring and evaluation procedures, the decision-making strategies continue to rank the MCDM problem alternatives similarly. These findings are congruent with what was described in previous research, displaying a robust array of decision-making techniques to be considered when assessing transportation infrastructure development. The results of this study further validate the design framework combining advanced MOO algorithms with MCDM techniques and provide new insights into its application and performance.

The subsequent sections detail and thoroughly explain the methodologies utilized in this study. Section 2.1 provides an overview of the RCPMF problem which serves as a standard for evaluating the effectiveness of the optimization algorithms. Section 2.2 elaborates on the operation and tailored adjustments of the optimization algorithms, while Section 2.3 offers similar clarification for the decision-making techniques. The analysis and interpretation of the results are presented in Section 3, enabling the formulation of relevant conclusions highlighted in Section 4.

2. Methods

This section provides a straightforward overview of the RCPMF problem used to assess the performance of optimization algorithms within the integrated MOO and MCDM life cycle design framework. Furthermore, it thoroughly delineates the optimization algorithms and defines the criteria weighting procedure and the decision-making techniques implemented in this research.

2.1. Optimization Problem Overview

This study builds upon the MOO problem in Ruiz-Vélez et al. [10], focusing on the structural design of a 10-m-span and 5-m-height RCPMF constructed 5 m deep into a roadway embankment. The MOO process involves determining a set of values for n variables constituting a solution vector $\vec{X}$ efficient per its corresponding values for predefined objective functions. These functions strive to achieve life cycle sustainability while adhering to constraints that prioritize structural integrity and performance. The ultimate aim is to navigate the solution space effectively, uncovering non-dominated solutions that simulta-

neously minimize k objective functions and meet m constraints. This approach follows the standard framework for MOO problems, as detailed by Equations (1)–(3).

$$\vec{X} = x_1, x_2, \ldots, x_n \tag{1}$$

$$min(f_i(\vec{X})) = min(f_1(\vec{X}), f_2(\vec{X}), \ldots, f_k(\vec{X})) \tag{2}$$

$$g_m(\vec{X}) \leq 0 \tag{3}$$

Section 2.1.1 outlines the variables and parameters relevant to the RCPMF problem, detailing the specific values and ranges utilized in the MOO process. Section 2.1.2 elaborates on the constraints that categorize a given variable vector as feasible or infeasible, integrating a concise overview of the constraint-verification process. This process encompasses checks for ultimate and serviceability limit states (ULS and SLS), which are crucial for assuring structural integrity and performance. Finally, Section 2.1.3 provides an exhaustive description of the three objective functions devised to assess economic viability along with environmental and social impacts at the life cycle endpoint.

2.1.1. Variables and Parameters

A set of 41 design variables defines the RCPMF design in the MOO problem in this study. These variables, represented in Figure 1, determine the structural geometry, the configuration of passive reinforcement, and the selection of material grades. In addition, a series of predetermined values are set as optimization parameters that reflect on the mechanical properties of materials, account for environmental conditions, adhere to legislative standards, or address specific design requirements related to the project's location.

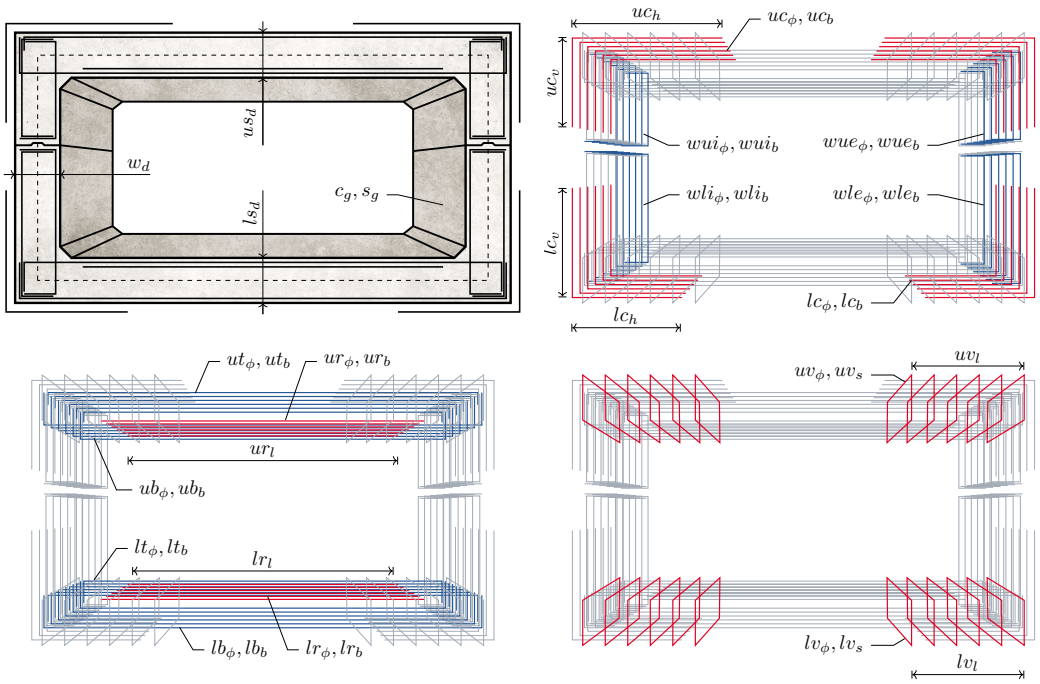

Figure 1. Optimization variables for the RCPMF design problem.

In exploring the MOO problem's solution landscape, the optimization algorithms systematically assign values within defined limits to the variables comprising the solution vector. This step is followed by assessing the objective functions for each solution set and a verification process to determine the solution's feasibility based on its adherence to the constraints. While variables are altered to explore potential designs during optimization, parameters—essential for fully delineating the design, objective function evaluation, and constraint verification—remain unchanged. Comprehensive modeling and testing of

the optimization process ensures a thorough exploration of viable solutions within the predetermined bounds of the optimization variables.

The RCPMF comprises three distinct types of optimization variables: real (continuous), choice (discrete), and integer. The MIP nature of the problem requires different handling for each during mutation, crossover, and repair operations throughout the optimization process. Given its notable efficacy when integrated with the NSGA-II algorithm, this study employs a statistical-based repair operator.

The RCPMF structural design is characterized by three continuous variables related to the depths of the upper and lower slabs and the lateral walls. Additionally, six continuous variables specify the effective lengths of passive reinforcement bars at the corners and within the central sections of both slabs. Four more continuous variables are allocated to determining the placement lengths of shear reinforcement in the slabs and their branch separation, summing up to thirteen continuous variables. Specific upper and lower bounds are defined for each continuous variable, allowing the optimization algorithm to select any value within this range throughout the optimization process.

Fourteen discrete variables are designated to specify the rebar diameters at all positions within the passive reinforcement layout. This approach is designed to be open-ended, permitting the optimization algorithm to consider unconventional designs by allowing rebar variables to adopt any standard diameter from 8, 10, 12, 14, 16, 20, 25, to 32 mm. Therefore, the discrete variables for rebar diameters are confined between 8 and 32 mm as their lower and upper bounds, respectively. Moreover, two discrete variables are introduced to select the grades for structural concrete and reinforcement steel, constrained to standard options of 25, 30, 35, and 40 MPa for concrete and 400 and 500 MPa for steel, offering a structured yet flexible framework for material selection.

Finally, a set of 12 integer variables contains the remaining data regarding the number of bars, which is necessary for fully defining the passive reinforcement design of the RCPMF. Handling the integer variables is relatively straightforward, requiring the establishment of specific lower and upper bounds. Following the above-mentioned non-restricting efforts, all integer variables are bounded within 4 to 20, corresponding to the minimum and maximum number of bars. The algorithm can then allocate any integer within said bounds for each variable. Table 1 compiles the full array of optimization variables, indicating their units, specific upper and lower bounds, and variable type.

When determining the structural integrity of an RCPMF, several critical aspects need consideration. These include the structure's geometric parameters, the properties of materials, and numerous indications per relevant standards, all essential for defining and modeling structural loads. Moreover, specific data are required to calculate objective function values for each feasible solution accurately. Table 2 summarizes these principal parameters, which equip the mathematical model with the necessary representativeness and precision for this analysis in combination with the optimization variables.

Table 1. Optimization problem variable units, bounds, and classification.

Variable	Unit	Lower Limit	Upper Limit	Type
us_d	m	0.60	1.60	continuous
ls_d	m	0.40	1.40	continuous
w_d	m	0.30	1.20	continuous
ut_ϕ	mm	8	32	discrete
ut_b	bars	4	20	integer
ub_ϕ	mm	8	32	discrete
ub_b	bars	4	20	integer
lt_ϕ	mm	8	32	discrete
lt_b	bars	4	20	integer
lb_ϕ	mm	8	32	discrete
lb_b	bars	4	20	integer
wui_ϕ	mm	8	32	discrete

Table 1. *Cont.*

Variable	Unit	Lower Limit	Upper Limit	Type
wui_b	bars	4	20	integer
wue_ϕ	mm	8	32	discrete
wue_b	bars	4	20	integer
wli_ϕ	mm	8	32	discrete
wli_b	bars	4	20	integer
wle_ϕ	mm	8	32	discrete
wle_b	bars	4	20	integer
uc_ϕ	mm	8	32	discrete
uc_b	bars	4	20	integer
uc_h	m	1	5	continuous
uc_v	m	0.70	1.80	continuous
lc_ϕ	mm	8	32	discrete
lc_b	bars	4	20	integer
lc_h	m	1	5	continuous
lc_v	m	0.70	2.80	continuous
ur_ϕ	mm	8	32	discrete
ur_b	bars	4	20	integer
ur_l	m	5	9.50	continuous
lr_ϕ	mm	8	32	discrete
lr_b	bars	4	20	integer
lr_l	m	3	8	continuous
uv_ϕ	mm	8	32	discrete
uv_s	m	0.1	0.4	continuous
uv_l	m	1.50	4.80	continuous
lv_ϕ	mm	8	32	discrete
lv_s	m	0.1	0.4	continuous
lv_l	m	1.50	4.80	continuous
c_g	MPa	25	40	discrete
s_g	MPa	400	500	discrete

Table 2. Optimization problem parameters and specific values.

Parameter	Unit	Value
Vertical height	m	5
Horizontal span	m	10
Hinge height	m	3
Embankment depth	m	5
Section depth	m	1
Terrain density	kN/m^3	20
Concrete density	kN/m^3	24
Steel density	kN/m^3	78.5
Terrain internal friction angle	°	30
Active earth pressure	–	0.33
Resting earth pressure	–	0.50
Heavy vehicle load	kN	150
Heavy vehicle length	m	1.20
Uniform overload	kN/m^2	10
Ballast coefficient	MN/m^3	10
Economic costs	EUR	Table 3
Environmental impact	point	Table 3
Social impact	mrh	Table 3
Standard regulations	CEN [22,23]/MFOM [24]	
Applicable codes	MFOM [25]	

2.1.2. Constraints

As with any structural design, the RCPMF solutions are deemed feasible based on compliance with standard regulations concerning ULS, SLS, and further considerations. The verification of these constraints was modeled and integrated within the Python 3-based model utilized for the optimization [26]. The mathematical model incorporates global Finite element method (FEM) models for stress analysis alongside several local models for sectional verification, ensuring a thorough examination of structural integrity and performance.

Achieving compliance with ULS is critical to ensuring the structural integrity of the RCPMF under various load cases as dictated by standard regulations. The ULS compliance check encompasses a multi-step process outlined in Algorithm 1. It begins with evaluating the shear stress resistance across the entire structure. Subsequently, it involves calculating the increase in bending moment stress due to shear interaction, which is then integrated into the overall stress analysis. Following this, the model computes the N-M interaction diagrams for each section, gaining detailed insight into the structural capacity at all sections of the RCPMF. This comprehensive analysis culminates in verifying normal stresses, explicitly checking if the combined axial-bending stress pair for each section falls within its N-M interaction diagram's safe region. A favorable evaluation across all sections indicates the RCPMF's capacity to withstand shear and normal stresses. The verification process also includes fatigue assessment and checks on geometrical configurations and reinforcement layouts. A design meeting all ULS requirements will be reflected in the optimization process as a constraint vector devoid of non-null values, signifying full compliance.

Algorithm 1 Constraint Verification for ULS

Function ULS_Verification(*model*)
Input: *model*—RCPMF Python model
Output: $ULS\_compliance\_vector$
$ULS\_compliance\_vector \leftarrow$ Array of size len($model.sections$)
Fill $ULS\_compliance\_vector$ with "non-compliant"
Conduct **Global FEM Analysis** on $model.global$
Initiate **ULS Local Analysis** on $model.sections$
for each $load\_case$ in $model.ULS\_load\_cases$ **do**
  for $section\_id$, $section$ in enumerate($model.sections$) **do**
    $shear \leftarrow section.shear\_stress \leq section.compute\_shear\_resistance()$
    $bending \leftarrow section.bending\_stress$ is within $section.compute\_N\_M\_interaction()$
    $fatigue \leftarrow section.fatigue\_stress \leq section.compute\_fatigue\_resistance()$
    $geometry \leftarrow section$ meets $model.regulation$ for geometry
    $reinforcement \leftarrow section$ meets $model.regulation$ for reinforcement layout
    if $shear$ AND $bending$ AND $fatigue$ AND $geometry$ AND $reinforcement$ **then**
      $ULS\_compliance\_vector[section\_id] \leftarrow$ "compliant"
    end if
  end for
end for
return $ULS\_compliance\_vector$

After verifying compliance with ULS, the assessment proceeds to SLS to ensure the structure not only remains safe under all relevant load cases but also retains its aesthetic and functional integrity. The SLS verification, outlined in Algorithm 2, is a multi-step process aimed at preventing crack formation and spread throughout the structure. Additionally, it limits displacements to prevent significant global deformations that might induce non-structural damage to the RCPMF's auxiliary systems. Analogous to the ULS procedure,

a design that satisfies all SLS criteria is represented by a constraint vector entirely free of non-zero values, indicating full adherence to serviceability requirements.

Algorithm 2 Constraint Verification for SLS

```
Function SLS_Verification(model)
Input: model – RCPMF Python model
Output: SLS_compliance_vector
SLS_compliance_vector ← Array of size len(model.sections)
Fill SLS_compliance_vector with "non-compliant"
Conduct Global FEM Analysis on model.global
Initiate SLS Local Analysis on model.sections
for each load_case in model.SLS_load_cases do
    displacement ← model.max_displacement meets model.regulations for displacements
    for section_id, section in enumerate(model.sections) do
        crack ← section.crack ≤ section.allowed_crack
        if crack AND displacement then
            SLS_compliance_vector[section_id] ← "compliant"
        end if
    end for
end for
return SLS_compliance_vector
```

2.1.3. Objective Functions

As delineated in the introductory paragraph of the section, the MOO process aims to identify a set of values for the n variables that compose $\vec{X}$. This set must comply with the constraints outlined in Section 2.1.2 while simultaneously minimizing the values of specific objective functions. The MOO problem focuses on achieving highly efficient RCPMF designs from a life cycle endpoint perspective. A comprehensive evaluation of RCPMF sustainability necessitates a clear definition and meticulous analysis of objective functions that reflect the complex dimensions of sustainability. Accordingly, the RCPMF MOO problem addressed in this study introduces three objective functions to assess the economic viability and the environmental and social ramifications throughout the RCPMF's life cycle, each contributing to a holistic sustainability evaluation.

During the optimization, all three objective functions are calculated through the Python mathematical model, taking into account the complete life cycle of the RCPMF. This approach entails defining parameters that encapsulate economic, environmental, and social data relevant to the materials and processes employed in the production, construction, upkeep, and eventual decommissioning of the RCPMF. In line with previous research, the economic analysis primarily evaluates the direct costs associated with concrete and steel, referencing prices from the BEDEC database [27]. For environmental and social impacts, the environmental life cycle assessment (ELCA) and social life cycle assessment (SLCA) endpoint results are determined by aggregating impacts across the RCPMF's four life cycle stages. This process is informed by unit impact values previously computed using OpenLCA 2.1, incorporating data from the Ecoinvent 3.7.1 and soca v2 databases, and analyzed through the ReCiPe 2008 and SWIM Life cycle impact assessment (LCIA) methodologies [28]. Table 3 specifies the specific values employed in the evaluation of objective functions [29–32].

Table 3. Material cost and life cycle environmental and social unit impact values [27–31].

Material	Unit	Cost (EUR)	$elca_i$ (Point)	$slca_i$ (mrh)
concrete 25 MPa	m^3	1.129×10^2	2.037×10^1	1.254×10^5
concrete 30 MPa	m^3	1.262×10^2	2.631×10^1	1.668×10^5
concrete 35 MPa	m^3	1.293×10^2	2.478×10^1	1.554×10^5
concrete 40 MPa	m^3	1.331×10^2	2.585×10^1	1.623×10^5
steel B400S	kg	1.790×10^0	2.417×10^{-1}	1.941×10^3
steel B500S	kg	1.840×10^0	2.538×10^{-1}	2.067×10^3
clay	kg	0.000×10^0	1.062×10^{-3}	8.475×10^0
gravel	kg	0.000×10^0	1.196×10^{-3}	2.617×10^0
sand	kg	0.000×10^0	1.718×10^{-3}	3.543×10^0
transport, lorry 16–32 ton	t·km	0.000×10^0	2.502×10^{-2}	4.116×10^1
transport, lorry 3.5–7.5 ton	t·km	0.000×10^0	7.755×10^{-2}	1.655×10^2
transport, car	km	0.000×10^0	2.760×10^{-4}	1.417×10^{-1}
digger, operation	min	0.000×10^0	7.876×10^{-2}	8.825×10^2
skid plate, operation	min	0.000×10^0	7.651×10^{-2}	8.657×10^2
diesel, building machine	MJ	0.000×10^0	1.361×10^{-2}	8.764×10^0
carbon dioxide	kg	0.000×10^0	4.369×10^{-2}	0.000×10^0
mortar	kg	0.000×10^0	3.084×10^{-2}	1.415×10^2
epoxy	kg	0.000×10^0	8.399×10^{-1}	4.107×10^3
rock crushing	kg	0.000×10^0	7.223×10^{-5}	8.304×10^{-1}

The first of the three objective functions is dedicated to assessing the economic cost of structural materials. The product of the unitary cost, c_i, and quantity used, m_i, for concrete and steel is added as per Equation (4).

$$C(\vec{X}) = \sum_{i=1}^{n} c_i \cdot m_i(\vec{X}) \tag{4}$$

The remaining two objective functions focus on the environmental and social ramifications of the RCPMF life cycle, analyzing the impacts from an endpoint perspective. A detailed analysis of every process throughout the RCPMF life cycle's four stages is conducted to calculate endpoint results, aligning with ISO 14040:2006 [33]. These stages are the manufacturing, construction, use and maintenance, and end-of-life. Additional insights into the life cycle model of the RCPMF, including discussions on the carbon capture capabilities of structural concrete, are elaborated in prior research [10].

The calculation for the ELCA endpoint results utilizes Equation (5). This formula aggregates the environmental impacts of materials and processes by multiplying each unit impact $elca_i$ by its corresponding quantity m_i, summing these across j life cycle stages. A parallel method, outlined in Equation (6), applies for calculating the SLCA endpoint results, ensuring both environmental and social impacts are comprehensively assessed.

$$ELCA(\vec{X}) = \sum_{i=1}^{n} \sum_{j=1}^{4} elca_{i,j} \cdot m_{i,j}(\vec{X}) \tag{5}$$

$$SLCA(\vec{X}) = \sum_{i=1}^{n} \sum_{j=1}^{4} slca_{i,j} \cdot m_{i,j}(\vec{X}) \tag{6}$$

2.2. Optimization Algorithms

This section introduces a framework for multi-objective optimization that includes the NSGA-II, NSGA-III, and RVEA algorithms. Section 2.2.1 is an initial setup involving a repair operator shared by all three methods, illustrating a consistent method for managing solutions. Detailed in Section 2.2.2 is the 'Algorithmic Enhancement Module' phase, in which the NSGA-II, NSGA-III, and RVEA algorithms are run. This approach allows for

the algorithms' performance to be directly compared, as discussed in Section 3.2, using measures such as generational distance and inverted generational distance. During this phase, unique operators tailored to each algorithm are employed, indicating the different strategies used for optimization. Figure 2 shows the standardized process and methods applied across these algorithms within the framework.

The enhancements detailed in our study include the application of a custom repair operator and specific tuning of the crossover and mutation operators, initially developed for NSGA-II and now extended to NSGA-III and RVEA. These adaptations enable a consistent application across different algorithms, enhancing their capability to address diverse optimization challenges. By integrating these tailored modifications into each algorithm, the framework facilitates a nuanced evaluation of their effectiveness in complex multi-objective environments.

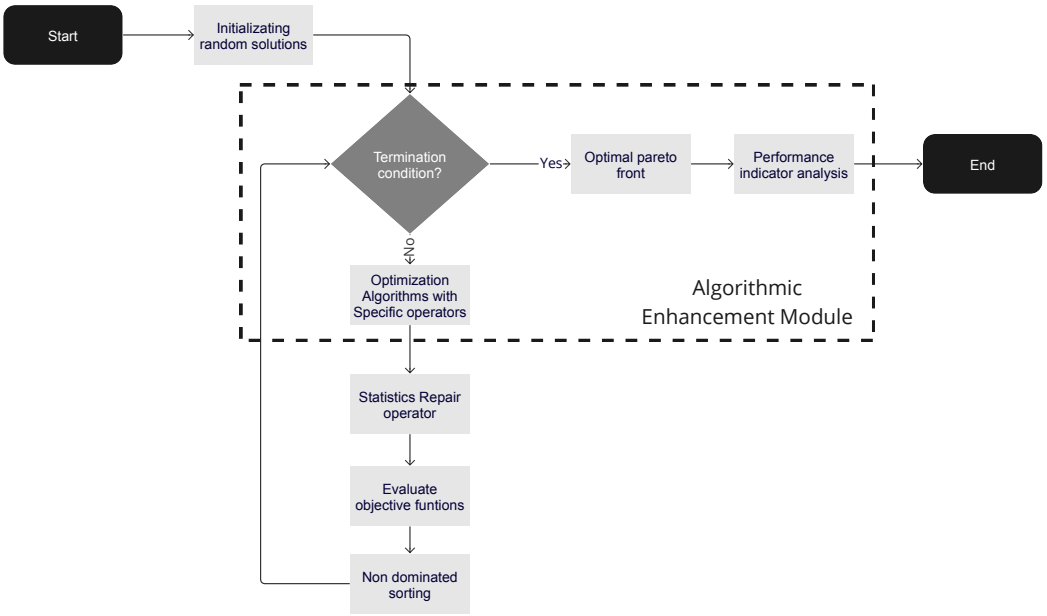

Figure 2. Flowchart depicting the framework with algorithmic enhancement module for NSGA-II, NSGA-III, and RVEA.

2.2.1. Statistical Repair Operator

A statistical-based repair operator, as outlined in Algorithm 3, is characterized by the integration of statistical measures—mean and median—with a probabilistic approach to enhance solutions in an optimization algorithm. In every iteration, solutions are processed using a probability parameter β to determine the chosen repair strategy. When a generated random number falls below β, the median is applied to discrete variables (choice and integer) and the mean to continuous (real) variables. The median is advantageous for discrete variables, providing resilience against outliers and representing the population's most common values. In contrast, the mean calculates an average value for continuous variables, capturing the population's central tendency.

Algorithm 3 Statistical Repair Operator

Function ProbabilisticRepair(Y, β)
Input: Y, β
Output: *repaired_Y*
repaired_Y ← copy of Y
average ← mean of Y along axis 0
midpoints ← median of Y along axis 0
for each solution y in *repaired_Y* **do**
  for each variable index i in y **do**
    varType ← variable type at index i
    if random number $< \beta$ **then**
      if *varType* is *Choice* or *Integer* **then**
        medianValue ← midpoints[i]
        if *varType* is *Choice* **then**
          $y[i]$ ← closest value to *medianValue* in *varType.choice*
        else
          $y[i]$ ← round *choice* to nearest integer within *var.bounds*
        end if
      else if *varType* is *Real* **then**
        $y[i]$ ← clip average[i] within *varType.bounds*
      end if
    else
      Standard repair is applied based on variable type and bounds
    end if
  end for
end for
return *repaired_Y*

2.2.2. Multi-Objective Optimization Algorithms

Custom NSGA-II: In the custom NSGA-II algorithm outlined in Algorithm 4, two pivotal operators are utilized: simulated binary crossover (SBX) and polynomial mutation (PM), each instrumental for strategic navigation within the search space. The SBX operator is finely tuned to generate offspring in close proximity to their parent solutions, fostering a concentrated exploration within the immediate vicinity of the solution space. Governed by a distribution index, it calibrates the closeness of the offspring to the parent solutions, striking a delicate balance between exploration and exploitation. Conversely, the PM operator introduces a subtle variation in the population by minutely altering the real-valued attributes of solutions. Similarly influenced by a distribution index, PM is essential for maintaining genetic diversity in the population and avoiding early convergence to suboptimal solutions. In concert, these operators propel the bespoke NSGA-II algorithm, ensuring a harmonious equilibrium between convergence to optimal solutions and diversity preservation, which is fundamental for the efficacy of multi-objective optimization.

Custom NSGA-III: In the elaboration of Custom NSGA-III, depicted in Algorithm 5, a strategic integration of selection, crossover, and mutation processes is employed to address complex many-objective optimization tasks. The algorithm adopts simulated binary crossover (SBX) and polynomial mutation (PM) to generate a diverse offspring pool, while a set of predefined reference directions aids in maintaining a well-distributed set of solutions across many objectives. This synergy of mechanisms distinguishes Custom NSGA-III from its predecessor, NSGA-II, by enhancing its capability to explore and exploit the multi-dimensional objective space. The reference-point-based selection strategy is particularly pivotal, effectively guiding the population towards a Pareto front that is representative

of the entire objective space, a critical aspect for many-objective optimization. The detailed procedure, as formalized in the provided pseudocode, encapsulates the algorithm's systematic approach towards achieving a comprehensive and diverse solution set.

Algorithm 4 Custom NSGA-II

Input: Population size pop_size, crossover probability $crossover\_prob$, mutation probability $mutation\_prob$, crossover distribution index $crossover\_index$, mutation distribution index $mutation\_index$
A set of non-dominated solutions
Initialize population P with pop_size individuals
Evaluate the initial population P
Set generation count $gen = 0$
while termination condition not met **do**
    Select parents from P using binary tournament selection
    Apply SBX crossover with probability $crossover\_prob$ and distribution index $crossover\_index$
    Apply PM mutation with probability $mutation\_prob$ and distribution index $mutation\_index$
    Evaluate the offspring population Q
    Combine populations: $R = P \cup Q$
    Perform non-dominated sorting on R
    Perform crowding distance assignment on each front
    Select the next generation population P from R
    $gen = gen + 1$
end while
return Population P containing non-dominated solutions

Algorithm 5 Custom NSGA-III

Input: Population size pop_size, crossover probability $crossover\_prob$, mutation probability $mutation\_prob$, crossover distribution index $crossover\_index$, mutation distribution index $mutation\_index$, reference directions ref_dirs
A set of non-dominated solutions distributed across the reference directions
Initialize population P with pop_size individuals
Evaluate the initial population P
Compute the reference points ref_dirs
Set generation count $gen = 0$
while termination condition not met **do**
    Select parents from P using tournament selection
    Apply SBX crossover with probability $crossover\_prob$ and distribution index $crossover\_index$
    Apply PM mutation with probability $mutation\_prob$ and distribution index $mutation\_index$
    Evaluate the offspring population Q
    Combine populations: $R = P \cup Q$
    Perform non-dominated sorting on R to get fronts $F_1, F_2, \ldots$
    Select the next generation population P using reference point based selection
    $gen = gen + 1$
end while
return Population P that approximates the Pareto front

Custom RVEA: In the development of the Custom RVEA, as outlined in Algorithm 6, elements are incorporated to effectively navigate and exploit the multi-objective optimization landscape. The algorithm leverages a set of reference directions (ref_dirs), which act as guiding vectors in the objective space, facilitating the distribution of solutions along the desired Pareto front. A novel feature, $prob\_neighbor\_mating$, introduces a mating preference

mechanism that enhances diversity and exploration by favoring mating between solutions that are neighbors, thereby ensuring a more thorough search across the entire solution space. Additionally, the adaptation parameter ($alpha$) dynamically adjusts the pressure exerted by the reference vectors, allowing for a flexible balance between convergence and diversity throughout the evolutionary process.

Algorithm 6 Custom RVEA with Specific Parameters

Input: Reference directions ref_dirs, number of neighbors $n\_neighbors$, probability of neighbor mating $prob\_neighbor\_mating$, adaptation parameter $alpha$, population size pop_size
A set of solutions approximating the Pareto front
Initialize population P with pop_size individuals
Evaluate the initial population P
Compute the reference vectors based on ref_dirs
Set generation count $gen = 0$
while termination condition not met **do**
    Assign each individual in P to a reference vector
    Calculate fitness of each individual based on angular distance to reference vectors and $alpha$
    Select parents, preferring those with closer neighbors with probability $prob\_neighbor\_mating$
    Generate offspring using crossover and mutation
    Evaluate the offspring
    Update the population P based on fitness and $alpha$ adaptation
    $gen = gen + 1$
end while
return Population P that approximates the Pareto front

2.3. Evaluation and Decision-Making Methods

The MOO introduced in Section 2.1 is tackled using the optimization algorithms described in Section 2.2. This approach yields a collection of non-dominated solutions indicative of highly efficient RCPMF designs. Embedding sustainability into the development of transportation infrastructure presents a multifaceted challenge. Therefore, this study broadens its examination beyond merely generating optimal designs that foster sustainability enhancements. It aims to assess and contrast the outcomes achieved through various decision-making strategies applied to the MCDM problem involving the highly efficient RCPMF designs result of the MOO. In this analysis, the subsequent phase of the design framework entails employing decision-making strategies to systematically and objectively rank the most effective design alternatives. Selecting a decision-making algorithm can turn into a MCDM problem itself. Within this context, the comparative analysis of the outcomes from each decision-making strategy aims to validate their use via a precise exploration of their utility in advancing sustainable development within transportation infrastructure.

Recognizing the vast considerations required for complex MCDM problems in any engineering field is crucial, especially given the sustainability-focused efforts of this research. Factors far exceeding the scope and objectives of this paper can profoundly impact the decision-making outcomes. With various conditions, including specific stakeholder interests, logistical and supply chain challenges, or temporary resource shortages, significantly shaping sustainable infrastructure development worldwide, this study acknowledges its limitations. The focus remains on examining the effectiveness of different decision-making algorithms and identifying the variances and parallels in their results for the RCPMF problem within the specific considerations outlined throughout the document.

Addressing the MCDM problem involves constructing a decision matrix $X = r_{ij}$ encompassing m alternatives $A_i = \{A_1, A_2, ..., A_m\}$, evaluated across n criteria. Element r_{ij} within this matrix offers insights into how well alternative i performs relative to criterion j. This study enhances previous research, applying five distinct decision-making algorithms:

SAW, FUCA, TOPSIS, PROMETHEE, and VIKOR. These algorithms necessitate initial criteria weighting as a preliminary step, providing essential information for their operation rather than being an intrinsic aspect of the algorithms.

2.3.1. Entropy Theory-Based Criteria Weighting

This paper utilizes entropy theory to calculate the criteria weights W_j for an objective and systematic approach to weighting [34]. This approach is crucial for maintaining the integrity of the analysis and mitigating the influence of subjective biases that could skew the results. Determining entropy weights unfolds in four stages. The initial step involves the normalization of X per Equation (7).

$$X' = r_{ij}\langle \sum_{i=1}^{m} r_{ij} \rangle^{-1} \tag{7}$$

The normalized matrix X' enables a direct comparison among criteria that, as seen in the MCDM problem of this study, may have different units and orders of magnitude. Entropy, indicative of a system's disorder, quantifies the requisite information to describe its state comprehensively. In this research, criteria exhibiting higher entropy are interpreted as yielding less reliable information, thereby influencing the decision-making efficiency of the algorithms. Subsequent steps in this methodology involve calculating the entropy E_j for each criterion and determining the degree of divergence D_j using Equations (8) and (9).

$$E_j = \frac{-1}{\ln\langle m \rangle} \left\langle \sum_{i=1}^{m} r_{ij} \cdot \ln\langle r_{ij} \rangle \right\rangle \tag{8}$$

$$D_j = 1 - E_j \tag{9}$$

The final step in the process calculates W_j by normalizing D_j across all criteria following Equation (10). These weights are subsequently utilized as input data for the decision-making algorithms, ensuring that each criterion's relative importance is accurately reflected in the analysis.

$$W_j = \frac{D_j}{\sum_{j=1}^{n} D_j} \tag{10}$$

2.3.2. Decision-Making Algorithms

The strategic selection of SAW, FUCA, TOPSIS, PROMETHEE, and VIKOR is founded on their capability to navigate the complexities and variances of decision-making scenarios encountered in MOO within sustainable engineering. Each MCDM technique offers a unique decision-making approach, strengthening the framework by utilizing diverse aspects of decision analysis, thus increasing the framework's overall robustness. The choice of these decision-making techniques enhances the decision-making process and ensures the framework's flexibility in accommodating different levels of data quality, stakeholder preferences, and sustainability criteria. This flexibility is essential for advancing the primary research goal of enhancing the robustness within the integrated application of MOO and MCDM.

SAW: The SAW technique streamlines decision-making by directly aggregating weighted criteria. This method provides a precise, quantitative evaluation of sustainability criteria, resulting in an immediate and explicit ranking of alternatives based on their aggregated scores. This paper integrates the SAW technique as a well-established and effective method that seamlessly integrates within the design framework, enhancing its efficiency and clarity in evaluating options.

Algorithm 7 depicts the operation of the SAW technique [35]. The SAW algorithm unfolds in three steps, initially computing the normalized decision matrix X'. After normalization, the S_i score for each alternative is evaluated as the sum of the products of each element r_{ij} and the entropy weight W_j across the criteria. The final phase involves

sorting them in ascending order based on the scores S, thereby identifying the most to least sustainable alternatives.

Algorithm 7 SAW Algorithm Implementation

Function SAW(X, W)
Input: X, W
Output: *ranking*
$S \leftarrow$ vector of zeros with size n
$X' \leftarrow$ normalize X along axis 0
for each alternative i in n **do**
  $S_i \leftarrow 0$
  for each criterion j in m **do**
    $r_{ij} \leftarrow X'_{ij}$
    $S_i \leftarrow S_i + W_j \cdot r_{ij}$
  end for
end for
ranking $\leftarrow$ sort S
return *ranking*

FUCA: The FUCA method ranks alternatives by systematically assessing them against multiple criteria. This approach considers the individual scores of each alternative and examines the distribution of these scores across various evaluations. FUCA's ability to effectively integrate and process variable data makes it a valuable tool in this study, supporting the goal of strengthening the robustness of the design framework for sustainable engineering solutions.

Algorithm 8 outlines the FUCA technique [14]. The FUCA starts by sorting alternatives in ascending order for each criterion. Following this, the score S_i results from aggregating the products of the rankings R_{ij} and the entropy weights W_j for all criteria. The concluding step involves a second sorting of the alternatives based on the ascending S scores.

Algorithm 8 FUCA Algorithm Implementation

Function FUCA(X, W)
Input: X, W
Output: *ranking*
$S \leftarrow$ vector of zeros with size n
for each alternative i in n **do**
  for each criterion j in m **do**
    $r_{ij} \leftarrow X_{ij}$
    $Q \leftarrow$ sort X_j
    $R_{ij} \leftarrow$ index of r_{ij} within Q
    $S_i \leftarrow S_i + W_j \cdot R_{ij}$
  end for
end for
ranking $\leftarrow$ sort S
return *ranking*

TOPSIS: The TOPSIS method assesses alternatives by measuring their distances to the most desirable (ideal) and least desirable (nadir) outcomes. Utilizing the Euclidean distance metric, TOPSIS ranks alternatives based on their geometric proximity to the ideal and their separation from the nadir. Focusing on optimal and suboptimal scenarios helps reduce the risk of selecting inferior solutions. Consequently, it ensures that the decision-

making process upholds the overarching goal of enhancing the robustness of the integrated design framework.

Algorithm 9 corresponds to the TOPSIS decision-making technique [36]. The TOPSIS algorithm also starts by computing the normalized decision matrix X'. The following step involves evaluating the normalized weighted matrix Tij. The next phase identifies the ideal and the least favorable solutions, A^+ and A^-, by pinpointing the highest and lowest values for each criterion j within T_{ij}.The essence of the TOPSIS algorithm is to measure how closely each alternative aligns with the ideal solution and how far it is from the least favorable one. This is achieved by determining the Euclidean distances D_i^+ and D_i^- of each alternative to the A^+ and A^- solutions, respectively. Following this, the algorithm evaluates the similarity index (S_i) as the ratio of the distance to the least favorable solution. In alignment with the previously described methods, the concluding step organizes the alternatives in descending order based on S.

PROMETHEE: The PROMETHEE method employs a pairwise comparison approach to rank alternatives, evaluating each option relative to others based on specific criteria and utilizing preference functions to ascertain the degree of preference for one alternative over another. The selection of PROMETHEE for this research is founded on its robust ability to accommodate both qualitative and quantitative criteria, promoting a thorough framework well-suited to the complexities of engineering decisions. This method facilitates nuanced decision-making, effectively capturing the subtle trade-offs and priorities essential to sustainable design and construction.

Algorithm 9 TOPSIS Algorithm Implementation

Function TOPSIS(X, W)
Input: X, W
Output: *ranking*
$S \leftarrow$ vector of zeros with size n
$X' \leftarrow$ normalize X along axis 0
for each criterion j in m **do**
    $T'_j \leftarrow X'_j \cdot W_j$
end for
$A^+, A^- \leftarrow \max(T'_j)$ and $\min(T'_j)$ for each criterion j in m
$D^+, D^- \leftarrow$ vectors of zeros with size n
for each alternative i in n **do**
    for each criterion j in m **do**
        $D_i^+ \leftarrow D_i^+ + (T'_{ij} - A_j^+)^2$
        $D_i^- \leftarrow D_i^- + (T'_{ij} - A_j^-)^2$
    end for
    $D_i^+ \leftarrow (D_i^+)^{0.5}$ distance to D^+
    $D_i^- \leftarrow (D_i^-)^{0.5}$ distance to D^-
    $S_i \leftarrow D_i^- / (D_i^- + D_i^+)$
end for
ranking $\leftarrow$ sort S
return *ranking*

Algorithm 10 illustrates the PROMETHEE method [37]. Initially, it constructs a preference matrix by comparing each pair of alternatives. This paper applies a preference function that quantifies the extent to which one alternative is preferred over another, factoring in the criteria weights W. This matrix is crucial for determining the positive and negative flows, Φ^+ and Φ^-, representing how much an alternative is preferred and opposed across all comparisons. The core of PROMETHEE lies in synthesizing these flows into a net flow Φ for each alternative, assessing its overall performance by offsetting its positive flow against

its negative. The procedure concludes with the alternatives ranked in descending net flow order, identifying the top choices. This systematic process, marked by pairwise preference aggregation, refines the decision matrix into an explicit hierarchy.

Algorithm 10 PROMETHEE Algorithm Implementation

Function: PROMETHEE(X, W)
Input: X, W
Output: *ranking*
$F \leftarrow$ matrix of zeros with size $n \times n$
for each alternative i in n **do**
  for each alternative j in n **do**
    if $i \neq j$ **then**
      $P_{ij} \leftarrow \max(0, X_i - X_j) \cdot W$
      $F_{ij} \leftarrow \sum P_{ij}$
    end if
  end for
end for
$\Phi^+, \Phi^- \leftarrow$ vectors of zeros with size n
for each alternative i in n **do**
  for each alternative j in n **do**
    $\Phi_i^+ \leftarrow \Phi_i^+ + F_{ij} \cdot (n-1)^{-1}$ positive flow
    $\Phi_i^- \leftarrow \Phi_i^- + F_{ji} \cdot (n-1)^{-1}$ negative flow
  end for
  $\Phi_i \leftarrow \Phi_i^+ - \Phi_i^-$ net flow
end for
ranking $\leftarrow$ sort Φ
return *ranking*

VIKOR: The VIKOR method ranks and selects alternatives by determining a compromise solution representing the closest agreement to the ideal. This method computes a utility measure for each alternative, reflecting the group utility, and a regret measure, indicating the individual regret of not achieving the ideal, to determine the rankings. VIKOR's methodological approach aligns well with the entropy-based weighting system used in the study, ensuring that the final decision reflects a balanced consideration of all relevant factors.

Algorithm 11 introduces the VIKOR method [38]. Initially, the VIKOR algorithm normalizes the decision matrix X to X'. It then identifies each criterion's best (f^+) and worst (f^-) performance values. For each alternative, the algorithm computes two metrics: S_i, the utility, calculated as the weighted sum of the distances from an alternative to the optimal solution, normalized by the total range of criterion values; and R_i, the regret, identifying the maximum of these normalized distances to indicate the furthest deviation from the optimal in the worst-case scenario. These measures are merged into a composite index Q_i using v, a balance coefficient to poise the overall group utility against individual regret. This paper considers a balance coefficient of 0.5 for this purpose. The final phase of VIKOR ranks the alternatives based on their Q values, effectively delineating the most from the least sustainable options.

Evaluating the outcomes of these five decision-making techniques allows for assessing the design framework's robustness. Further, by examining the set of non-dominated solutions resulting from the MOO problem, this approach directly evaluates the efficacy of the NSGA-II, NSGA-III, and RVEA optimization algorithms in identifying high-quality optimums within the intricate solution space of the RCPMF problem. Consequently, this enhances the existing knowledge of their capabilities in promoting sustainable structural design and validates its integration with one or several decision-making algorithms.

Algorithm 11 VIKOR Algorithm Implementation

Function VIKOR(X, W)
Input: X, W
Output: *ranking*
$X' \leftarrow$ normalize X along axis 0
$f^+, f^- \leftarrow \max(X'_j)$ and $\min(X'_j)$ for each criterion j in m
$S, R \leftarrow$ vectors of zeros with size n
for each alternative i in n **do**
  for each criterion j in m **do**
    $S_i \leftarrow S_i + W_j \cdot (f_j^+ - X'_{ij}) \cdot (f_j^+ - f_j^-)^{-1}$
    $R_i \leftarrow \max(R_i, W_j \cdot (f_j^+ - X'_{ij}) \cdot (f_j^+ - f_j^-)^{-1})$
  end for
end for
$S^* \leftarrow \min(S)$, $S^- \leftarrow \max(S)$
$R^* \leftarrow \min(R)$, $R^- \leftarrow \max(R)$
$Q \leftarrow$ vector of zeros with size n
for each alternative i in n **do**
  $Q_i \leftarrow vs. \cdot (S_i - S^*)/(S^- - S^*) + (1 - v) \cdot (R_i - R^*)/(R^- - R^*)$
end for
ranking $\leftarrow$ sort Q
return *ranking*

3. Results

This section presents the outcomes of deploying optimization algorithms on the RCPMF problem and the subsequent decision-making approach. Section 3.1 analyzes each MOO algorithm's effectiveness in generating non-dominated solutions equivalent to highly efficient, sustainable designs. Subsequently, Section 3.3 delves into evaluating the MCDM problem concerning ranking optimal solutions derived from the MOO.

3.1. Algorithm Comparisons

The tuning process for the crossover and mutation operators within the NSGA-II algorithm was conducted methodically in two phases, with the hypervolume metric serving as the primary evaluation criterion. For the calculation of the hypervolume, each configuration was executed five times. In the initial exploratory phase, a range of η values—0.2, 0.5, and 0.9—were examined to assess their impact on offspring distribution relative to their parent solutions, applied to both the SBX and PM operators. Furthermore, the probabilities for these operators were tested across a range of values—0.01, 0.1, 0.2, and 0.3—to find a wide variety of potential settings aimed at improving the optimization efforts. This was followed by an exploitation phase considering values 0.1, 0.08, 0.06, 0.04, and 0.02. This stage aimed to find an initial setup that could support a balanced approach to exploration and exploitation in the multi-objective optimization environment.

Following the same structured approach, the tuning process was extended to the NSGA-III algorithm, adhering to the established η and probability values to ensure consistency in the evaluation. For NSGA-III, the final η value was settled at 0.5 after a comprehensive assessment, mirroring the decision-making process in NSGA-II. In the probability tuning phase, an expanded range of values—0.01, 0.03, 0.04, 0.05, 0.06, and 0.07—was investigated, ultimately selecting 0.05 as the optimal setting. Additionally, the partitioning count for determining reference directions was fixed at 12, aiming to capture a broad diversity of solution directions and thus enriching the algorithm's ability to uniformly cover the Pareto front.

The tuning methodology was applied to the RVEA algorithm, with an emphasis on the conceptual underpinnings of the parameters being adjusted. Initially, the process focused on the probability of mating between neighboring solutions, exploring values of 0.2, 0.5, and 0.8, before refining the search to 0.15, 0.2, 0.25, and 0.3 in a subsequent phase. The optimal value was determined to be 0.2, highlighting the algorithm's preference for

exploiting local solution neighborhoods to enhance diversity and exploration. Similarly, the adaptation of the algorithm's convergence rate, guided by the conceptually defined adaptation parameter, was explored through initial values of 1.0, 1.5, and 2.0, with further refinement to 2.1, 2.0, and 1.9. A final value of 2.0 was selected, underscoring the balance achieved between fast convergence and the maintenance of solution diversity over generations. The setting for the number of partitions used to determine the distribution of reference directions was maintained at 12, mirroring the approach in NSGA-III and ensuring a consistent framework for analysis. In the table shown in Table 4, the different configurations tested, along with the optimal values identified for each parameter, are presented.

Table 4. Tuning summary of NSGA-II, NSGA-III, and RVEA algorithms using hypervolume as a factor to identify the best outcome.

Algorithm	Parameter	Tested Values	Optimal Value
NSGA-II	η (SBX & PM)	0.2, 0.5, 0.9	0.5
	Probability	0.02, 0.04, 0.06, 0.08, 0.1, 0.2, 0.3	0.02
NSGA-III	η	0.2, 0.5, 0.9	0.5
	Probability	0.01, 0.03, 0.04, 0.05, 0.06, 0.07	0.05
	Partition count	-	12
RVEA	Probability of mating	0.2, 0.5, 0.8, 0.15, 0.2, 0.25, 0.3	0.2
	Adaptation parameter	1.0, 1.5, 2.0, 2.1, 2.0, 1.9	2.0
	Partition count	-	12

Table 5 showcases the quantitative analysis of the non-dominated solutions generated by the NSGA-II, NSGA-III, and RVEA optimization algorithms for the MOO problem. It includes the specific values of the objective functions for each design, facilitating an objective assessment of each algorithm's performance based on three criteria: cost, ELCA, and SLCA.

Table 5. Multi-objective optimization results for each algorithm.

Algorithm	Cost (EUR)	ELCA (Point)	SLCA (mrh)
NSGA-II	5.92679×10^3	1.64259×10^3	9.04790×10^6
NSGA-II	5.69768×10^3	1.69912×10^3	9.27121×10^6
NSGA-II	5.74080×10^3	1.65304×10^3	8.96734×10^6
NSGA-III	4.78051×10^3	1.44901×10^3	7.20000×10^6
NSGA-III	4.51830×10^3	1.52920×10^3	7.65131×10^6
NSGA-III	5.03727×10^3	1.50440×10^3	7.00960×10^6
RVEA	5.23727×10^3	1.51671×10^3	8.09550×10^6
RVEA	5.19441×10^3	1.41667×10^3	8.24518×10^6
RVEA	5.34868×10^3	1.54679×10^3	8.05434×10^6

This study utilizes an adapted min–max normalization technique to address the disparities in measurement units and magnitude scales across the evaluation criteria. In this framework, the radar charts depicted in Figure 3 illustrate the performance of each algorithm against the three evaluation metrics, applying this normalized approach. The adjusted normalization method sets a baseline of 0.5 for the lowest value and a cap of 1 for the highest value in the dataset. In this setup, radar charts with smaller areas indicate superior performance by the algorithms. This superior performance is indicative of RCPMF designs that exhibit enhanced sustainability throughout their life cycle.

The analysis of the multi-objective optimization results, presented in Table 5 and Figure 3, underscores the performance of the NSGA-II, NSGA-III, and RVEA algorithms across three critical objectives: cost, environmental life cycle analysis (ELCA), and social life cycle analysis (SLCA). The findings are instrumental in elucidating the algorithms'

efficiencies and shortcomings in navigating the complex multi-objective landscape of sustainable infrastructure projects.

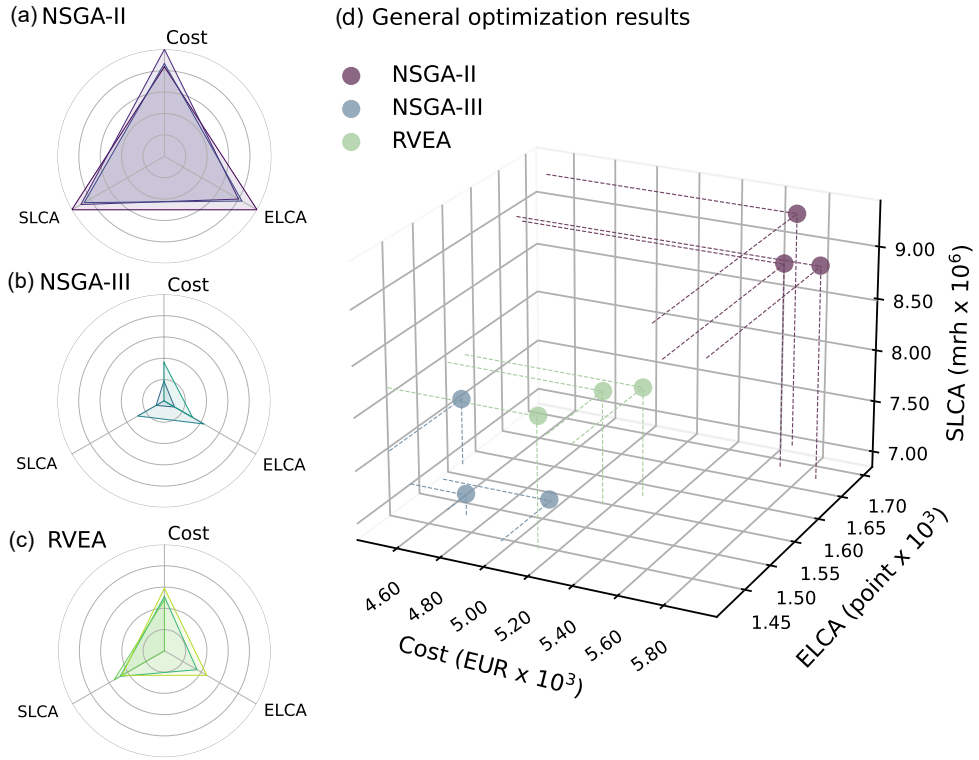

Figure 3. Algorithm comparison across three objective functions: (**a**) normalized NSGA-II, (**b**) normalized NSGA-III, (**c**) normalized RVEA, and (**d**) general algorithm performance in terms of cost (EUR), ELCA (point), and SLCA (mrh).

It was observed that NSGA-II consistently yielded the least favorable outcomes across all three objectives, indicating a relative underperformance in integrating cost efficiency with environmental and social sustainability metrics. In contrast, NSGA-III emerged as the most adept in minimizing costs and achieving superior SLCA outcomes compared to RVEA, suggesting a robust capability in optimizing for economic and social dimensions simultaneously. The distinction in performance between NSGA-III and RVEA became particularly pronounced when examining their ability to balance cost reduction with social sustainability, with NSGA-III demonstrating a more effective optimization pathway. Meanwhile, RVEA displayed good performance in the ELCA domain, albeit with outcomes closely rivaled by NSGA-III, highlighting its effectiveness in environmental sustainability optimization with marginally superior ELCA values. This nuanced performance profile underscores RVEA's potential in addressing environmental aspects of sustainability, albeit within a competitive margin when juxtaposed with NSGA-III.

3.2. Performance Indicator Analysis

This study conducted a systematic experiment to assess the performance of three multi-objective optimization algorithms: NSGA-II, NSGA-III, and RVEA. The experiment consisted of 30 separate runs, during which five points were generated for each algorithm using the same predefined parameters. This methodology allowed for the direct comparison of the algorithms' performance under fixed parameter settings. A min–max normalization procedure was applied to each function separately to ensure comparability among the results from different objective functions. This method involved standardizing the units of the variables for all data points, including those on the Pareto frontier. For each experiment, points from each algorithm were normalized by adjusting their values from the minimum to the maximum observed across the dataset. This process facilitated a consistent com-

parison across different optimization landscapes by transforming the varied scales into a uniform metric.

Two performance metrics were introduced to evaluate further the effectiveness of the optimization algorithms: generational distance (GD) and inverted generational distance (IGD). Both metrics quantify the quality of the solutions generated by the algorithms in terms of their convergence and diversity concerning a known Pareto frontier.

Generational distance (GD) quantifies the average Euclidean distance from each solution in a set to the nearest point in the Pareto front, reflecting the convergence of the algorithm-generated solutions. For this paper's experiment, the size of set A was 5, representing the five points obtained in each run. The GD is calculated using the following equation:

$$GD(A) = \left(\frac{1}{5} \sum_{i=1}^{5} (d_i^2) \right)^{\frac{1}{2}}$$

where d_i is the Euclidean distance from the i-th solution a_i in set A to its nearest point in the Pareto front Z. Here, A and Z are defined as follows:

$$A = \{a_1, a_2, \ldots, a_5\}, \quad Z = \{z_1, z_2, \ldots, z_{|Z|}\}.$$

This measure is pivotal for assessing the proximity of the obtained solutions to the ideal solutions on the Pareto front.

Inverted generational distance (IGD) inverts the generational distance and measures the distance from any point in Z, the Pareto front, to the closest point in A. For this paper's experiment, set A contained five points generated in each run. The IGD is calculated using the following equation:

$$IGD(Z) = \left(\frac{1}{|Z|} \sum_{i=1}^{|Z|} (\hat{d}_i^2) \right)^{\frac{1}{2}}$$

where $\hat{d}_i$ is the Euclidean distance (with $p = 2$) from a point z_i in the Pareto front to its nearest reference point in set A. The set A is defined as $A = \{a_1, a_2, \ldots, a_5\}$, representing the solutions obtained from each run. This metric is crucial for evaluating how well the generated set of solutions covers the Pareto front.

Advantages of Each Metric:

- **GD** is particularly useful for assessing the convergence of the generated solutions to the Pareto front. A lower GD value indicates that the algorithm-generated solutions are closer to the optimal set of solutions, suggesting better performance in terms of convergence.
- **IGD** offers insight into the convergence and diversity of the generated solutions. It shows how close the solutions are to the Pareto front and how well the solutions are distributed across the entire front. A lower IGD value signifies that the generated solutions uniformly cover the Pareto front, indicating a good spread in addition to proximity.

By incorporating both GD and IGD, this study evaluates the algorithms' ability to generate solutions that are close to and well-distributed across the ideal solution set, capturing the nuanced performance differences between the algorithms in multi-objective optimization tasks.

Descriptive statistics were computed, providing basic insights into the distribution of results for each algorithm to evaluate the performance of the optimization algorithms. These included the mean, standard deviation, maximum, minimum, and median values, essential for summarizing the central tendency and dispersion of the data. Furthermore, the non-parametric Kruskal–Wallis test was employed to ascertain statistically significant differences between the algorithms. This test was chosen due to its robustness in han-

dling non-normally distributed data and its ability to compare more than two groups without assuming equal variances, making it well-suited for the ordinal data generated in this experiment.

In Table 6, the descriptive statistics reveal patterns in the performance of the MOO algorithms NSGA-II, NSGA-III, and RVEA. Regarding generational distance (GD), NSGA-III and RVEA display similar mean values, indicating comparable proficiency in converging to the Pareto front. This similarity is also reflected in the median and standard deviation values, suggesting consistent performance across the 30 experiments. On the other hand, a pronounced difference is observed for inverted generational distance (IGD). NSGA-III presents a substantially lower mean and median compared to RVEA, highlighting its enhanced capability to generate a diverse set of solutions that effectively span the entire Pareto front.

The non-parametric Kruskal–Wallis test was conducted to statistically affirm the differences in performance observed between the algorithms, as detailed in Table 6. This test is ideal for data that do not follow a normal distribution, which often happens in the case of multi-objective optimization because it compares the median values across groups without assuming data normality. The resulting *p*-values for both average generational distance (Avg GD) (1.29×10^{-13}) and inverted generational distance (IGD) (6.59×10^{-18}) were significantly low, leading to the rejection of the null hypothesis and confirming differences in algorithm performance. The results indicate that NSGA-III may be more effective in generating a diverse set of solutions, as demonstrated by its IGD results.

Table 6. Results of GD and IGD for various algorithms across experiments.

Experiment	**GD**			**IGD**		
	NSGA-II	NSGA-III	RVEA	NSGA-II	NSGA-III	RVEA
1	0.9664	0.1292	0.0803	0.9904	0.2348	0.3808
2	1.1340	0.1481	0.1411	1.1619	0.2332	0.3784
3	1.0045	0.1446	0.1585	1.0451	0.2529	0.4040
4	0.9965	0.1473	0.1649	1.0108	0.2353	0.3645
5	0.9698	0.1307	0.1207	1.0364	0.2456	0.3426
6	0.9280	0.1646	0.1637	1.0216	0.2630	0.3281
7	1.0534	0.1377	0.1285	1.0095	0.2308	0.3363
8	0.9312	0.1602	0.1236	0.9675	0.2456	0.3999
9	1.0279	0.1439	0.1100	1.0708	0.2088	0.3326
10	1.0039	0.0922	0.1418	1.0574	0.2283	0.3736
11	0.9841	0.1511	0.1540	0.9471	0.2505	0.3859
12	1.0160	0.1127	0.1062	1.0275	0.2276	0.4011
13	0.9124	0.1421	0.1101	0.9132	0.2248	0.3524
14	1.0595	0.1332	0.1593	1.0609	0.2242	0.3418
15	1.0723	0.1619	0.1378	1.0425	0.2533	0.3504
16	1.0322	0.1222	0.1239	1.0990	0.2283	0.3710
17	0.9758	0.1384	0.1359	0.9857	0.2270	0.3422
18	1.0865	0.1748	0.1186	1.0432	0.2433	0.3254
19	1.0100	0.1614	0.1290	0.9320	0.2634	0.3570
20	1.0245	0.1132	0.1392	1.0530	0.2236	0.3336
21	1.0509	0.0986	0.1460	1.1170	0.2397	0.3483
22	1.0935	0.1298	0.1329	1.1163	0.2362	0.3871
23	1.0668	0.1190	0.1615	1.0783	0.2398	0.4041
24	0.9923	0.1247	0.1603	1.0493	0.2368	0.3667
25	1.0751	0.1264	0.1212	1.0994	0.2288	0.3500
26	0.9908	0.0817	0.1362	1.0070	0.2435	0.3412
27	0.9587	0.1581	0.1603	0.9125	0.2582	0.4232
28	1.0647	0.1084	0.1573	1.0251	0.2343	0.3747
29	1.0590	0.1223	0.1274	1.0541	0.2556	0.3851
30	0.9676	0.1280	0.1158	0.9620	0.2351	0.3446
Mean	1.0169	0.1336	0.1355	1.0299	0.2384	0.3642
Std Dev	0.0528	0.0219	0.0203	0.0598	0.0127	0.0259
Max	1.1340	0.1748	0.1649	1.1619	0.2634	0.4232
Min	0.9124	0.0817	0.0803	0.9125	0.2088	0.3254
Median	1.0130	0.1320	0.1361	1.0395	0.2358	0.3608
Kruskal–Wallis *p*-value		1.29×10^{-13}			6.59×10^{-18}	

3.3. Multi-Criteria Decision Analysis for Structural Design Optimization

This paper comprehensively evaluates the efficacy of the NSGA-II, NSGA-III, and RVEA optimization algorithms within a structural design context. This section presents the analysis of the non-dominated solutions produced by each optimization algorithm in addressing the RCPMF challenge. Additionally, the results of deploying a comprehensive range of decision-making methods are examined to gauge the applicability of these techniques within the structural design framework and the robustness and replicability of its results, considering both optimization and MCDM perspectives.

Within this context, Table 7 presents the collection of optimization variables that delineate the non-dominated solutions. The configuration of passive reinforcement—encompassing aspects like diameter, the amount of bars, and separation of shear branches—is combined into an effective area A_{re} parameter. This method facilitates its interpretation, offering direct insight into the sectional properties and streamlining the comprehension of these elements.

Figure 4 showcases the primary geometric features of the upper and bottom slabs and the lateral walls for the structures yielded by each optimization algorithm. Across all the alternatives, optimal designs feature upper slab depths ranging between 0.75 and 1.07 m, with the RVEA algorithm exhibiting the most significant variability in its results. The NSGA-II algorithm, in particular, favors designs that incorporate wider lower slabs, reaching up to 0.93 m. This tendency towards increased lower slab depths is not as pronounced in the non-dominated solutions produced by NSGA-III and RVEA, which tend towards more moderate section depths, averaging 0.65 and 0.71 m, respectively. Despite the distinct variability observed in the designs of the upper and lower slabs, a consistent pattern emerges among all three optimization algorithms, converging on solutions with specified lateral wall depths, thereby narrowing the variability across these sections of the RCPMF.

Table 7. Non-dominated solution optimization variables for each optimization algorithm.

	NSGA-II			**NSGA-III**			**RVEA**		
	A_1	A_2	A_3	A_4	A_5	A_6	A_7	A_8	A_9
w_d	3.89×10^{-1}	3.89×10^{-1}	4.28×10^{-1}	3.08×10^{-1}	3.01×10^{-1}	3.00×10^{-1}	3.80×10^{-1}	3.58×10^{-1}	3.54×10^{-1}
us_d	8.31×10^{-1}	8.31×10^{-1}	$1.02 \times 10^{+0}$	7.84×10^{-1}	$1.06 \times 10^{+0}$	8.29×10^{-1}	7.86×10^{-1}	7.53×10^{-1}	$1.07 \times 10^{+0}$
ls_d	9.25×10^{-1}	9.25×10^{-1}	6.51×10^{-1}	6.01×10^{-1}	6.58×10^{-1}	7.05×10^{-1}	6.43×10^{-1}	8.29×10^{-1}	6.60×10^{-1}
A_{wli}	2.20×10^{-3}	2.20×10^{-3}	1.61×10^{-3}	2.95×10^{-3}	4.02×10^{-3}	1.21×10^{-3}	3.93×10^{-3}	3.93×10^{-3}	2.51×10^{-3}
A_{wle}	1.01×10^{-3}	1.01×10^{-3}	3.14×10^{-3}	1.21×10^{-3}	5.50×10^{-4}	1.24×10^{-3}	5.65×10^{-4}	7.07×10^{-4}	1.01×10^{-3}
A_{wui}	1.13×10^{-3}	1.13×10^{-3}	1.41×10^{-3}	2.95×10^{-3}	7.85×10^{-4}	1.41×10^{-3}	2.41×10^{-3}	2.45×10^{-3}	1.26×10^{-3}
A_{wue}	2.83×10^{-3}	2.83×10^{-3}	2.20×10^{-3}	7.07×10^{-4}	8.04×10^{-4}	1.96×10^{-3}	1.02×10^{-3}	1.88×10^{-3}	4.71×10^{-4}
A_{ub}	6.38×10^{-3}	6.38×10^{-3}	4.42×10^{-3}	4.71×10^{-3}	4.08×10^{-3}	4.42×10^{-3}	4.91×10^{-3}	3.93×10^{-3}	4.42×10^{-3}
A_{ur}	2.41×10^{-3}	2.41×10^{-3}	4.40×10^{-3}	2.41×10^{-3}	3.02×10^{-3}	4.40×10^{-3}	3.77×10^{-3}	2.81×10^{-3}	4.42×10^{-3}
A_{ut}	1.24×10^{-3}	1.24×10^{-3}	5.50×10^{-4}	8.64×10^{-4}	3.93×10^{-4}	2.01×10^{-3}	1.01×10^{-3}	6.28×10^{-4}	8.04×10^{-4}
A_{lb}	1.96×10^{-3}	1.96×10^{-3}	1.41×10^{-3}	2.45×10^{-3}	7.92×10^{-4}	1.13×10^{-3}	1.26×10^{-3}	1.88×10^{-3}	8.04×10^{-4}
A_{lr}	8.84×10^{-3}	8.84×10^{-3}	3.02×10^{-3}	7.36×10^{-3}	1.81×10^{-3}	3.42×10^{-3}	3.42×10^{-3}	1.92×10^{-3}	2.04×10^{-3}
A_{lt}	1.47×10^{-3}	1.47×10^{-3}	2.61×10^{-3}	2.01×10^{-3}	1.36×10^{-3}	8.64×10^{-4}	2.61×10^{-3}	7.85×10^{-4}	5.40×10^{-3}
A_{lc}	5.65×10^{-4}	5.65×10^{-4}	1.61×10^{-3}	3.14×10^{-4}	3.14×10^{-4}	1.88×10^{-3}	1.01×10^{-3}	7.92×10^{-4}	7.92×10^{-4}
A_{uc}	1.36×10^{-3}	1.36×10^{-3}	8.04×10^{-4}	1.61×10^{-3}	5.65×10^{-4}	9.42×10^{-4}	1.26×10^{-3}	4.52×10^{-4}	1.96×10^{-3}
A_{uv}	3.42×10^{-3}	3.42×10^{-3}	2.50×10^{-3}	1.81×10^{-3}	1.44×10^{-3}	4.68×10^{-3}	3.27×10^{-3}	5.16×10^{-3}	3.36×10^{-3}
A_{lv}	1.00×10^{-3}	8.97×10^{-4}	5.24×10^{-3}	1.08×10^{-3}	5.84×10^{-3}	8.60×10^{-4}	2.84×10^{-3}	7.67×10^{-4}	8.48×10^{-4}
lc_v	$2.73 \times 10^{+0}$	$2.73 \times 10^{+0}$	$1.29 \times 10^{+0}$	$1.08 \times 10^{+0}$	$2.18 \times 10^{+0}$	$1.50 \times 10^{+0}$	$1.24 \times 10^{+0}$	$2.02 \times 10^{+0}$	$1.20 \times 10^{+0}$
lc_h	$4.71 \times 10^{+0}$	$4.71 \times 10^{+0}$	$4.07 \times 10^{+0}$	$3.57 \times 10^{+0}$	$3.20 \times 10^{+0}$	$3.92 \times 10^{+0}$	$3.07 \times 10^{+0}$	$4.43 \times 10^{+0}$	$4.69 \times 10^{+0}$
uc_v	$1.00 \times 10^{+0}$	$1.00 \times 10^{+0}$	$1.24 \times 10^{+0}$	$1.27 \times 10^{+0}$	$1.51 \times 10^{+0}$	$1.62 \times 10^{+0}$	$1.51 \times 10^{+0}$	$1.15 \times 10^{+0}$	$1.14 \times 10^{+0}$
uc_h	$1.52 \times 10^{+0}$	$1.52 \times 10^{+0}$	$2.01 \times 10^{+0}$	$1.51 \times 10^{+0}$	$4.59 \times 10^{+0}$	$4.06 \times 10^{+0}$	$2.46 \times 10^{+0}$	$3.53 \times 10^{+0}$	$2.04 \times 10^{+0}$
uv_l	$3.19 \times 10^{+0}$	$3.19 \times 10^{+0}$	$3.63 \times 10^{+0}$	$3.03 \times 10^{+0}$	$3.22 \times 10^{+0}$	$3.70 \times 10^{+0}$	$3.03 \times 10^{+0}$	$3.06 \times 10^{+0}$	$4.24 \times 10^{+0}$
lv_l	$3.14 \times 10^{+0}$	$2.81 \times 10^{+0}$	$2.42 \times 10^{+0}$	$3.67 \times 10^{+0}$	$1.22 \times 10^{+0}$	$2.94 \times 10^{+0}$	$3.42 \times 10^{+0}$	$1.07 \times 10^{+0}$	$2.52 \times 10^{+0}$
ur_l	$9.55 \times 10^{+0}$	$9.55 \times 10^{+0}$	$5.29 \times 10^{+0}$	$7.95 \times 10^{+0}$	$7.96 \times 10^{+0}$	$7.64 \times 10^{+0}$	$7.26 \times 10^{+0}$	$8.58 \times 10^{+0}$	$7.04 \times 10^{+0}$
lr_l	$9.06 \times 10^{+0}$	$9.11 \times 10^{+0}$	$5.20 \times 10^{+0}$	$6.69 \times 10^{+0}$	$9.01 \times 10^{+0}$	$5.19 \times 10^{+0}$	$5.88 \times 10^{+0}$	$6.15 \times 10^{+0}$	$5.13 \times 10^{+0}$
c_g	$3.50 \times 10^{+1}$	$3.00 \times 10^{+1}$	$3.50 \times 10^{+1}$	$3.50 \times 10^{+1}$	$2.50 \times 10^{+1}$	$3.50 \times 10^{+1}$	$3.50 \times 10^{+1}$	$3.50 \times 10^{+1}$	$2.50 \times 10^{+1}$
s_g	$4.00 \times 10^{+2}$	$4.00 \times 10^{+2}$	$5.00 \times 10^{+2}$	$5.00 \times 10^{+2}$	$5.00 \times 10^{+2}$	$5.00 \times 10^{+2}$	$4.00 \times 10^{+2}$	$5.00 \times 10^{+2}$	$4.00 \times 10^{+2}$

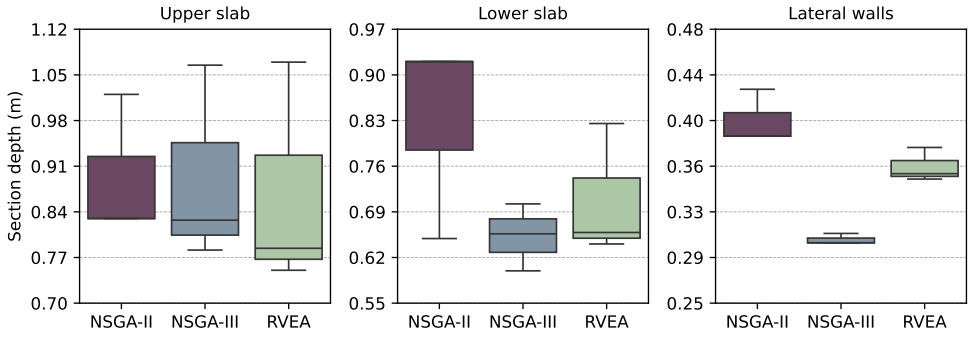

Figure 4. Sectional geometry comparison of the non-dominated solutions for each algorithm.

Figure 5 portrays the analysis of the use of material resources for each non-dominated solution derived from the NSGA-II, NSGA-III, and RVEA optimization algorithms. Notably, the NSGA-III and RVEA algorithms lead to designs that consume less concrete. This trend correlates with the more pronounced sectional depths in solutions from NSGA-III for the RCPMF. Moreover, NSGA-III tends to converge towards designs that make more efficient use of passive reinforcement, thereby reducing the required mass of steel. In contrast, the NSGA-II algorithm exhibits less favorable outcomes in this regard, with its solutions generally demanding higher quantities of concrete and steel resources. Despite these differences, all solutions maintain passive reinforcement densities exceeding 100 kg/m^3. Within this spectrum, the NSGA-III algorithm trends towards solutions with somewhat lower reinforcement densities, whereas NSGA-II and RVEA display closely aligned results in terms of structural material usage.

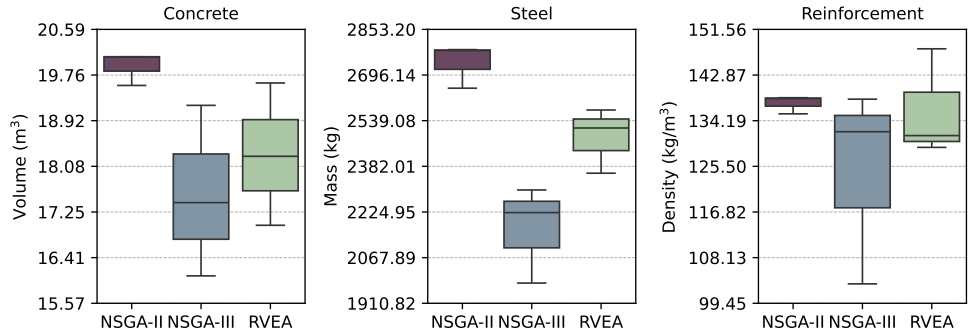

Figure 5. Structural material comparison of the non-dominated solutions for each algorithm.

This manuscript comprehensively evaluates the NSGA-II, NSGA-III, and RVEA algorithms, focusing on their proficiency in generating non-dominated optimal solutions within a MOO for the RCPMF design challenge. Section 3.1 meticulously explored how these optimization algorithms perform against three sustainability metrics pertinent to the life cycle of the RCPMF. Previous paragraphs detailed the primary attributes of the RCPMF designs. This paper now critically assesses the design framework integrating MOO algorithms with MCDM approaches. Table 8 analyzes the results of deploying the SAW, FUCA, TOPSIS, PROMETHEE, and VIKOR decision-making algorithms on the MCDM problem, explicitly focusing on ranking the non-dominated solutions generated from the MOO process.

Table 8. Multi-criteria decision-making for structural optimization results.

	Cost	ELCA	SLCA	Scores					Ranks				
W_j	**0.33368**	**0.33165**	**0.33467**	S_i^S	S_i^F	S_i^T	S_i^P	S_i^V	R_i^S	R_i^F	R_i^T	R_i^P	R_i^V
A_1	5.92×10^3	1.64×10^3	9.04×10^6	0.9809	8.0020	0.8964	0.9014	0.9728	8	8	8	8	8
A_2	5.69×10^3	1.69×10^3	9.27×10^6	0.9871	8.3326	0.9019	1.0000	1.0000	9	9	9	9	9
A_3	5.74×10^3	1.65×10^3	8.96×10^6	0.9657	7.6653	0.8609	0.8657	0.8441	7	7	7	7	7
A_4	4.78×10^3	1.44×10^3	7.20×10^6	0.8118	2.0000	0.1366	0.0840	0.0000	1	1	1	2	1
A_5	4.51×10^3	1.52×10^3	7.65×10^6	0.8310	2.9959	0.2420	0.2834	0.2244	3	3	2	3	3
A_6	5.03×10^3	1.50×10^3	7.00×10^6	0.8296	2.3306	0.2424	0.0000	0.1550	2	2	3	1	2
A_7	5.23×10^3	1.51×10^3	8.09×10^6	0.8831	4.6683	0.4696	0.4801	0.3307	5	5	5	5	5
A_8	5.19×10^3	1.41×10^3	8.24×10^6	0.8666	3.6743	0.4322	0.5462	0.2988	4	4	4	6	4
A_9	5.34×10^3	1.54×10^3	8.05×10^6	0.8937	5.3306	0.5117	0.4619	0.4178	6	6	6	4	6

The radar plot featured in Figure 6 employs the modified min–max normalization technique to represent the scoring outcomes of the nine alternatives utilizing the five distinct decision-making techniques. This methodology bypasses the scoring disparities inherent to the varied algorithmic structures of these techniques. Despite their operational discrepancies, the scoring outcomes from the five decision-making approaches exhibit remarkable uniformity across all alternatives. This consistency is further observed in the correlation heatmap, which effectively highlights the strong correlation among the five decision-making techniques.

The entropy-based weighting showcases a commendable equilibrium among the three life cycle assessment metrics, underscoring the importance of cost, ELCA, and SLCA in informing the decision-making process. The scoring outcomes reveal significant similarity in how the five decision-making techniques score and rank the alternatives, with correlation coefficients exceeding 0.94. This high correlation denotes a substantial uniformity in evaluation outcomes despite the inherent differences in each algorithm's methodology. Interestingly, this consensus is particularly pronounced among the highest and lowest-ranked alternatives, whereas the most noticeable discrepancies in ranking occur among those in the middle. This pattern suggests a decision-making framework that effectively differentiates between the most and least sustainable options, with slight variations observed among the moderately performing alternatives.

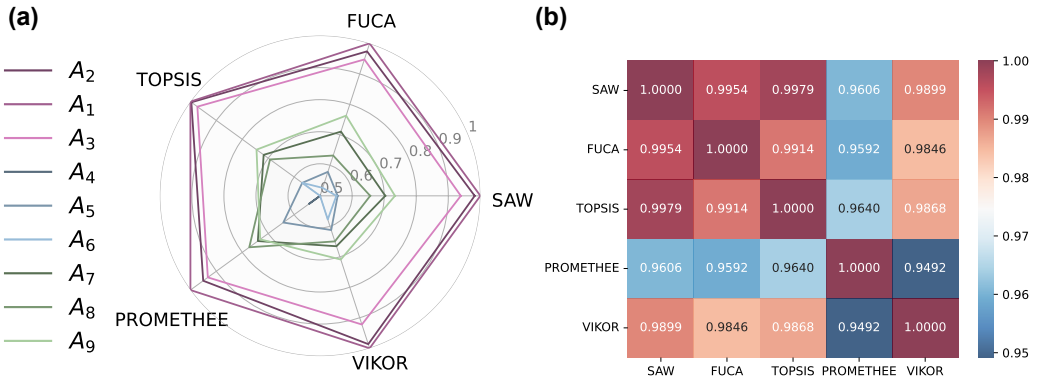

Figure 6. Decision-making algorithm result comparison: (**a**) radar plot with normalized alternative scores, and (**b**) scoring correlation across all decision-making algorithms (SAW, FUCA, TOPSIS, PROMETHEE, and VIKOR).

Alternatives A_4 to A_6, representing the non-dominated solutions produced by the NSGA-III algorithm, consistently emerge as the top three selections for the MCDM problem. Notably, alternative A_4 is deemed the highest-ranked RCPMF design by four decision-making techniques, with only PROMETHEE favoring A_6 as the leading option. On the

other end of the spectrum, alternatives A_1 to A_3, derived from the NSGA-II algorithm, are identified as the least favorable options. Each technique unambiguously categorizes these RCPMF designs as offering minimal life cycle sustainability benefits within highly efficient structures. This observation does not detract from their efficiency but underscores the NSGA-III's superior compatibility with the RCPMF within the outlined MOO framework. Meanwhile, the alternatives A_7 to A_9, generated by the RVEA algorithm, occupy the intermediate positions in the ranking.

The high correlation among the outcomes derived from the five decision-making algorithms highlights the replicability and reliability of the methodology that combines MOO and MCDM within the design framework for the RCPMF challenge. This section provided an in-depth assessment of the performance of various MOO algorithms in developing RCPMF designs that prioritize life cycle sustainability. Further, by applying a range of decision-making techniques, this analysis scrutinized the efficacy of the NSGA-II, NSGA-III, and RVEA algorithms, endorsing their incorporation into a cohesive structural design framework combining MOO and MCDM. This holistic strategy demonstrates the decision-making process's integrity, validates the integrated design framework capabilities, and extends the range of techniques available to advance sustainable structural design methodologies.

4. Conclusions

This paper critically evaluates the life cycle optimization performance of three optimization algorithms within a cohesive design framework that integrates for advancing sustainable transportation infrastructure. Combining MOO techniques with MCDM methodologies, this work expands upon and substantiates a systematic approach to addressing the intricate challenges in efficient structural engineering design. The investigation employs the RCPMF design problem, leveraging an array of MOO algorithms: NSGA-II, NSGA-III, and RVEA. These algorithms are enhanced with specialized crossover, mutation, and statistical-based repair operators to address the MIP nature of the MOO problem. The algorithms' performance is evaluated against life cycle sustainability metrics—economic cost, ELCA, and SLCA—across every non-dominated solution. The analysis highlights the NSGA-III as the best-performing algorithm, offering a nuanced understanding of its potential to facilitate sustainable design approaches.

Following the optimization phase, the MCDM problem is rigorously evaluated, addressing nine non-dominated solutions generated by the optimization algorithms. This study utilizes a comprehensive set of decision-making techniques, including SAW, FUCA, TOPSIS, PROMETHEE, and VIKOR, coupled with an entropy theory-based methodology for unbiased criteria weighting. This combination further enhances the framework's capabilities in identifying efficient designs. The results corroborate and expand the methods available for a cohesive MOO and MCDM design framework, demonstrating the strategy's efficiency and reliability. Such findings advocate for a transformative approach to infrastructure development, steering towards more advanced and sustainable engineering solutions.

- NSGA-III is highlighted as the most effective algorithm, with its non-dominated solutions for the RCPMF designs consistently ranked as the top three choices by all applied decision-making techniques. RVEA positions next, with its solutions ranked in the mid-range, yet exhibiting some of the best scores for life cycle sustainability metrics.
- On the other end, NSGA-II shows less favorable outcomes for RCPMF optimization within the defined framework of this study, pointing towards its limited applicability under the examined conditions. This evaluation outlines the relative performance of each algorithm, contributing valuable insights into their suitability for addressing the specific characteristics of the RCPMF problem within sustainable transportation infrastructure design.
- The analysis of performance indicators has offered insights into the potential efficacy of the NSGA-II, NSGA-III, and RVEA algorithms. Descriptive statistics, based on 30 experimental runs, suggest that NSGA-III is relatively consistent in its approach towards

the Pareto front, as reflected by its similar mean and GD values when compared to RVEA. In the case of IGD, NSGA-III appears to have an edge, hinting at its capability to produce a more varied set of solutions. The Kruskal–Wallis test lends statistical support to these observations, suggesting significant differences in performance among the algorithms.

- In addressing the MCDM problem, a significant alignment is observed in the ranking of alternatives by the five decision-making algorithms despite the intrinsic differences in their algorithmic structure and scoring methodologies. This concurrence, represented by correlation coefficients from 0.94 to 0.99, underscores the robustness of the decision-making process within the integrated MOO and MCDM frameworks, demonstrating a cohesive understanding and evaluation of the alternatives' sustainability performances.
- Four out of five decision-making algorithms identified the alternative A_4 as the most sustainable design for the RCPMF over its life cycle. This design utilizes 35 MPa structural concrete to construct slender lateral walls and features restrained section depths for both the upper and lower slabs. Although it does not secure the lowest values in cost, ELCA, or SLCA, the design effectively leverages B500S steel for passive reinforcement, conforming to a well-rounded design. This outcome emphasizes the necessity of an integrated approach that employs MOO to address multiple aspects of sustainability simultaneously.
- By applying and critically evaluating the design framework for the RCPMF optimization problem, this study aims to validate and expand upon a practical method for incorporating life cycle considerations right from the design phase. The findings underscore the effectiveness and reliability of combining MOO and MCDM techniques. This integrated approach aims to produce economically viable designs that excel in environmental and social sustainability across their life cycle. These solutions signify a significant stride towards embedding holistic sustainability criteria in structural design processes.

While the outcomes align with previous research and further underscore the efficacy and robustness of integrating MOO with MCDM, the authors recognize the limitations arising from the assumptions and premises articulated throughout this study. These constraints were essential to develop a comprehensive mathematical model capable of facilitating the design process, including structural calculation, constraint verification, objective function assessment, and exploration of the optimization landscape. Additionally, considering the modular nature of the structural solution, integrating factors related to supply chain and transportation challenges could lay the groundwork for further evaluating the scalability of the specific case study discussed in this paper. Given the focus on sustainable infrastructure development, the authors consider these additions a crucial direction for future research efforts. Nonetheless, these factors delineate the scope of the present investigation. Future work that delves into varied scenarios, optimization benchmarks, and data variability holds promise for refining this approach, potentially broadening its applicability and enhancing its precision in structural design optimization.

Given the observed variances in the convergence and diversity metrics among the NSGA-II, NSGA-III, and RVEA algorithms, future studies should thoroughly investigate the underlying mechanisms contributing to these differences. A detailed examination of algorithmic parameters, such as selection pressure, mutation rates, and crossover strategies, could provide insights into their impact on convergence behaviors. Additionally, exploring the interaction between these parameters and the specific problem characteristics of the RCPMF designs might reveal why certain algorithms outperform others in specific contexts. Pursuing these inquiries could lead to more tailored algorithmic adjustments that enhance performance across a broader range of optimization scenarios, optimizing the algorithms for specific types of multi-objective problems.

Author Contributions: Conceptualization, A.R.-V. and J.G.; methodology, A.R.-V., J.G., J.A. and V.Y.; software, A.R.-V. and J.G.; validation, A.R.-V., J.A. and V.Y.; formal analysis, A.R.-V.; investigation, A.R.-V. and J.G.; resources, A.R.-V., J.A. and V.Y.; data curation, A.R.-V.; writing—original draft preparation, A.R.-V.; writing—review and editing, J.G., J.A. and V.Y.; visualization, A.R.-V.; supervision, J.A. and V.Y.; project administration, V.Y.; funding acquisition, V.Y. All authors have read and agreed to the published version of the manuscript.

Funding: Grant PID2020-117056RB-I00 funded by MCIN/AEI/10.13039/501100011033 and by "ERDF A way of making Europe".

Data Availability Statement: All the data used in the research can be found in the article.

Conflicts of Interest: The authors declare no conflicts of interest.

Abbreviations

The following abbreviations are used in this manuscript:

SOO	Single-objective optimization
MOO	Multi-objective optimization
RCPMF	Reinforced concrete precast modular frame
NSGA-II	Non-dominated sorting genetic algorithm II
MIP	Mixed-integer programming
MCDM	Multi-criteria decision-making
SAW	Simple additive weighting
FUCA	Faire un choix adéquat
NSGA-III	Non-dominated sorting genetic algorithm III
RVEA	Reference vector guided evolutionary algorithm
ELCA	Environmental life cycle analysis
SLCA	Social life cycle analysis
TOPSIS	Technique for order of preference by similarity to ideal solution
PROMETHEE	Preference ranking organization method for enrichment evaluation
VIKOR	Visekriterijumska optimizacija i kompromisno resenje
ULS	Ultimate limit state
SLS	Service limit state
FEM	Finite element method
ELCA	Environmental life cycle assessment
SLCA	Social life cycle assessment
LCIA	Life cycle impact assessment
SBX	Simulated binary crossover
PM	Polynomial mutation
GD	Generational distance
IGD	Inverted generational distance

References

1. Kyriacou, A.P.; Muinelo-Gallo, L.; Roca-Sagalés, O. The efficiency of transport infrastructure investment and the role of government quality: An empirical analysis. *Transp. Policy* **2019**, *74*, 93–102. [CrossRef]
2. WCED. *Our Common Future*; World Commission on Environment and Development: Oxford, UK, 1987.
3. Favier, A.; De Wolf, C.; Scrivener, K.; Habert, G. *A Sustainable Future for the European Cement and Concrete Industry: Technology Assessment for Full Decarbonisation of the Industry by 2050*; Technical Report; ETH Zurich: Zürich, Switzerland, 2018.
4. Santoro, J.F.; Kripka, M. Evaluation of CO_2 emissions in RC structures considering local and global databases. *Innov. Infrastruct. Solut.* **2024**, *9*, 33. [CrossRef]
5. Yepes, V.; Medina, J. Economic heuristic optimization for heterogeneous fleet VRPHESTW. *J. Transp. Eng.* **2006**, *132*, 303–311. [CrossRef]
6. Spangenberg, J.H.; Fuad-Luke, A.; Blincoe, K. Design for Sustainability (DfS): The interface of sustainable production and consumption. *J. Clean. Prod.* **2010**, *18*, 1485–1493. [CrossRef]
7. Zhang, Z.; Cheng, X.; Xing, Z.; Gui, X. Pareto multi-objective optimization of metro train energy-saving operation using improved NSGA-II algorithms. *Chaos Solitons Fractals* **2023**, *176*, 114183. [CrossRef]

8. Lahmar, S.; Maalmi, M.; Idchabani, R. Multiobjective building design optimization using an efficient adaptive Kriging metamodel. *Simulation* **2023**. [CrossRef]
9. Rastegaran, M.; Beheshti Aval, S.; Sangalaki, E. Multi-objective reliability-based seismic performance design optimization of SMRFs considering various sources of uncertainty. *Eng. Struct.* **2022**, *261*, 114219. [CrossRef]
10. Ruiz-Vélez, A.; García, J.; Alcalá, J.; Yepes, V. Sustainable Road Infrastructure Decision-Making: Custom NSGA-II with Repair Operators for Multi-Objective Optimization. *Mathematics* **2024**, *12*, 730. [CrossRef]
11. Ruiz-Vélez, A.; Alcalá, J.; Yepes, V. Optimal design of sustainable reinforced concrete precast hinged frames. *Materials* **2023**, *16*, 204. [CrossRef]
12. Ruiz-Vélez, A.; Alcalá, J.; Yepes, V. A parametric study of optimum road modular hinged frames by hybrid metaheuristics. *Materials* **2023**, *16*, 931. [CrossRef]
13. Blank, J.; Deb, K. pymoo: Multi-Objective Optimization in Python. *IEEE Access* **2020**, *8*, 89497–89509. [CrossRef]
14. Zakeri, S.; Chatterjee, P.; Konstantas, D.; Ecer, F. A comparative analysis of simple ranking process and faire un Choix Adéquat method. *Decis. Anal. J.* **2024**, *10*, 100380. [CrossRef]
15. Levitt, T. *Exploit the Product Life Cycle*; Graduate School of Business Administration, Harvard University: Cambridge, MA, USA, 1985.
16. Deb, K.; Pratap, A.; Agarwal, S.; Meyarivan, T. A fast and elitist multiobjective genetic algorithm: NSGA-II. *IEEE Trans. Evol. Comput.* **2002**, *6*, 182–197. [CrossRef]
17. Blank, J.; Deb, K.; Roy, P.C. Investigating the Normalization Procedure of NSGA-III. In Proceedings of the Evolutionary Multi-Criterion Optimization, East Lansing, MI, USA, 10–13 March 2019; Springer International Publishing: Berlin/Heidelberg, Germany, 2019; pp. 229–240.
18. Cheng, R.; Jin, Y.; Olhofer, M.; Sendhoff, B. A Reference Vector Guided Evolutionary Algorithm for Many-Objective Optimization. *IEEE Trans. Evol. Comput.* **2016**, *20*, 773–791. [CrossRef]
19. Tanhadoust, A.; Madhkhan, M.; Nehdi, M.L. Two-stage multi-objective optimization of reinforced concrete buildings based on non-dominated sorting genetic algorithm (NSGA-III). *J. Build. Eng.* **2023**, *75*, 107022. [CrossRef]
20. Muñoz-Medina, B.; Ordóñez, J.; Romana, M.G.; Lara-Galera, A. Typology Selection of Retaining Walls Based on Multicriteria Decision-Making Methods. *Appl. Sci.* **2021**, *11*, 1457. [CrossRef]
21. Navarro, I.J.; Yepes, V.; Martí, J.V. A Review of Multicriteria Assessment Techniques Applied to Sustainable Infrastructure Design. *Adv. Civ. Eng.* **2019**, *2019*, 6134803. [CrossRef]
22. CEN. *Eurocode 2: Design of Concrete Structures*; European Comittee for Standarization: Brussels, Belgium, 2013.
23. CEN. *Eurocode 1: Actions on Structures*; European Comittee for Standarization: Brussels, Belgium, 2009.
24. MFOM. *IAP-11: Code on the Actions for the Design of Road Bridges*; Ministerio de Fomento: Madrid, Spain, 2011.
25. MFOM. *Guía de Cimentaciones en Obra de Carretera*; Ministerio de Fomento: Madrid, Spain, 2009.
26. Van Rossum, G.; Drake, F.L. *Python 3 Reference Manual*; CreateSpace: Scotts Valley, CA, USA, 2009.
27. BEDEC. Catalonia Institute of Construction Technology. BEDEC ITEC Materials Database. Available online: https://metabase.itec.cat/vide/es/bedec (accessed on 8 January 2024).
28. Goedkoop, M.; Heijungs, R.; Huijbregts, M.; De Schryver, A.; Struijs, J.; Van Zelm, R. *ReCiPe 2008. Report I: Characterisation*; Ministry of Housing, Spatial planning and Environment (VROM): Barendrecht, The Netherlands, 2009; pp. 1–44.
29. Frischknecht, R.; Rebitzer, G. The ecoinvent database system: A comprehensive web-based LCA database. *J. Clean. Prod.* **2005**, *13*, 1337–1343. [CrossRef]
30. Soca v. 2 add-on: Adding social impact information to ecoinvent. In *Description of Methodology to Map Social Impact Information from PSILCA v3 to Ecoinvent v. 3.7.1*; GreenDelta GmbH: Berlin, Germany, 2021.
31. Ciroth, A.; Eisfeldt, F. PSILCA – A product social impact life cycle assessment database. *Database Version* **2016**, *1*, 1–99.
32. Ciroth, A. ICT for environment in life cycle applications OpenLCA—A new open source software for Life Cycle Assessment. *Int. J. Life Cycle Assess.* **2007**, *12*, 209. [CrossRef]
33. *ISO 14040:2006*; Environmental Management, Life Cycle Assessment Principles and Framework. International Organization for Standardization: Geneva, Switzerland, 2006.
34. Zeleny, M. *Multiple Criteria Decision Making*; McGraw-Hill: New York, NY, USA, 1982.
35. Churchman, C.W.; Ackoff, R.L. An Approximate Measure of Value. *J. Oper. Res. Soc. Am.* **1954**, *2*, 172–187. [CrossRef]
36. Hwang, C.L.; Lai, Y.J.; Liu, T.Y. A new approach for multiple objective decision making. *Comput. Oper. Res.* **1993**, *20*, 889–899. [CrossRef]
37. Behzadian, M.; Kazemzadeh, R.; Albadvi, A.; Aghdasi, M. PROMETHEE: A comprehensive literature review on methodologies and applications. *Eur. J. Oper. Res.* **2010**, *200*, 198–215. [CrossRef]
38. Opricovic, S.; Tzeng, G.H. Compromise solution by MCDM methods: A comparative analysis of VIKOR and TOPSIS. *Eur. J. Oper. Res.* **2004**, *156*, 445–455. [CrossRef]